บทบาทของเคอร์คิวมินต่อการเปลี่ยนแปลงการแสดงออกของพีพาร์แกมมา การกระตุ้นเอ็นเอฟแคปปาบี และภาวะออกซิเดทีฟสเตรสในหนูแรทที่ตับอักเสบจากแอลกอฮอล์

นางสาว สุจิตรา สมุหเสนีโต

วิทยานิพนธ์นี้เป็นส่วนหนึ่งของการศึกษาตามหลักสูตรปริญญาวิทยาศาสตรดุษฎีบัณฑิต
สาขาวิชาสรีรวิทยา (สหสาขาวิชา)
บัณฑิตวิทยาลัย จุฬาลงกรณ์มหาวิทยาลัย
ปีการศึกษา 2551

ROLE OF CURCUMIN ON CHANGES OF PPARγ EXPRESSION, NF-κB ACTIVATION AND OXIDATIVE STRESS IN RATS WITH ALCOHOLIC HEPATITIS

Miss Suchittra Samuhasaneeto

A Dissertation Submitted in Partial Fulfillment of the Requirements
for the Degree of Doctor of Philosophy Program in Physiology
(Interdisciplinary Program)
Graduate School
Chulalongkorn University
Academic Year 2009

Thesis Title	Role of Curcumin on Changes of PPARγ Expression, NF-κB Activation and Oxidative Stress in Rats with Alcoholic Hepatitis
By	Miss Suchittra Samuhasaneeto
Field of Study	Physiology
Advisor	Associate Professor Duangporn Thong-Ngam, M.D.
Co-Advisor	Associate Professor Onanong Kulaputana, M.D., Ph.D.

Accepted by the Graduate School, Chulalongkorn University in Partial Fulfillment of the Requirements for the Doctoral Degree

.....Dean of the Graduate School
(Associate Professor Pornpote Piumsomboon, Ph.D.)

THESIS COMMITTEE

..... Chairman
(Associate Professor Prakong Tangpraprutigul, Ph.D.)

..... Advisor
(Associate Professor Duangporn Thong-Ngam, M.D.)

..... Co-Advisor
(Associate Professor Onanong Kulaputana, M.D., Ph.D.)

..... Examiner
(Associate Professor Juraiporn Somboonwong, M.D.)

..... Examiner
(Associate Professor Kris Angkanaporn, D.V.M., Ph.D.)

..... Examiner
(Associate Professor Pisit Tangkijvanich, M.D.)

..... External Examiner
(Bubpha Pornthisarn, M.D.)

สุจิตรา สมุหเสนีโต : บทบาทของเคอร์คิวมินต่อการเปลี่ยนแปลงการแสดงออกของพีพาร์แกมมา การกระตุ้นเอ็นเอฟแคปปาบี และภาวะออกซิเดทีฟสเตรสในหนูแรทที่ตับอักเสบจากแอลกอฮอล์. (ROLE OF CURCUMIN ON CHANGES OF PPARγ EXPRESSION, NF-κB ACTIVATION AND OXIDATIVE STRESS IN RATS WITH ALCOHOLIC HEPATITIS) อ.ที่ปรึกษาวิทยานิพนธ์หลัก : รศ. พญ. ดวงพร ทองงาม, อ.ที่ปรึกษาวิทยานิพนธ์ร่วม : รศ.ดร.พญ. อรอนงค์ กุละพัฒน์, 109 หน้า.

แอลกอฮอล์ออกซิเดชั่นทำให้เกิดสารจากกระบวนการสันดาปที่เป็นพิษและเหนี่ยวนำให้เกิดภาวะออกซิเดทีฟสเตรสซึ่งสนับสนุนต่อพยาธิสภาพการเกิดโรคตับจากแอลกอฮอล์ เคอร์คิวมินเป็นสารออกฤทธิ์จากพืช *Curcuma longa* Linn. ซึ่งมีฤทธิ์ต้านอนุมูลอิสระและต้านการอักเสบ การศึกษาครั้งนี้เพื่อหากลไกที่เป็นไปได้ของเคอร์คิวมินที่สามารถลดตับอักเสบจากแอลกอฮอล์ในหนูแรท โดยทำการทดลองในหนูแรทเพศเมียสายพันธุ์ Spraque-Dawley แบ่งเป็น 4 กลุ่มโดย กลุ่มควบคุมได้รับน้ำกลั่น กลุ่มแอลกอฮอล์ได้รับแอลกอฮอล์ 50% ขนาด 7.5 กรัม/กิโลกรัม/วัน และกลุ่มเคอร์คิวมินได้รับเคอร์คิวมินขนาด 400 มิลลิกรัม/กิโลกรัม/วัน หรือ 1,200 มิลลิกรัม/กิโลกรัม/วัน ซึ่งละลายในแอลกอฮอล์ 50% ขนาด 7.5 กรัม/กิโลกรัม/วัน โดยได้รับแอลกอฮอล์หรือเคอร์คิวมินโดยทาง Intragastric tube เป็นเวลา 4 สัปดาห์ เมื่อสิ้นสุดการทดลองเก็บตัวอย่างตับ ผลการทดลองในกลุ่มแอลกอฮอล์พบพยาธิสภาพของตับมีไขมันสะสมในเซลล์ตับระดับน้อยถึงปานกลาง มีการอักเสบและการตายของเซลล์ตับน้อย ระดับมาลอนไดอัลดีไฮด์ในตับ การตายของเซลล์ตับแบบอะพ็อพโทซิส และการกระตุ้นเอ็นเอฟแคปปาบีสูงขึ้นอย่างมีนัยสำคัญเปรียบเทียบกับกลุ่มควบคุม ส่วนกลุ่มเคอร์คิวมินพบพยาธิสภาพของตับดีขึ้น ลดระดับที่เพิ่มขึ้นของมาลอนไดอัลดีไฮด์ในตับและยับยั้งการกระตุ้นเอ็นเอฟแคปปาบี ส่วนการทำงานของเอ็นไซม์ซุปเปอร์ออกไซด์ดิสมิวเตสกับการแสดงออกของโปรตีนพีพาร์แกมมาไม่มีความแตกต่างในทุกกลุ่ม กลุ่มเคอร์คิวมินขนาด 400 มิลลิกรัม/กิโลกรัม/วัน มีแนวโน้มลดการตายของเซลล์ตับแบบอะพ็อพโทซิส สรุปผลการทดลองเคอร์คิวมินสามารถลดตับอักเสบจากแอลกอฮอล์โดยผ่านทางลดภาวะออกซิเดทีฟสเตรสและยับยั้งการกระตุ้นเอ็นเอฟแคปปาบี และอาจจะมีแนวโน้มลดการตายของเซลล์ตับแบบอะพ็อพโทซิส ส่วนการแสดงออกของโปรตีนพีพาร์แกมมาอาจจะไม่เปลี่ยนแปลงในระยะแรกของตับอักเสบจากแอลกอฮอล์

สาขาวิชา สรีรวิทยา ลายมือชื่อนิสิต สุจิตรา

ปีการศึกษา 2551 ลายมือชื่ออ.ที่ปรึกษาวิทยานิพนธ์หลัก

ลายมือชื่ออ.ที่ปรึกษาวิทยานิพนธ์ร่วม

4989703220 : MAJOR PHYSIOLOGY

KEYWORDS : CURCUMIN / OXIDATIVE STRESS / NF-κB / RATS WITH ALCOHOLIC HEPATITIS

SUCHITTRA SAMUHASANEETO : ROLE OF CURCUMIN ON CHANGES OF PPARγ EXPRESSION, NF-κB ACTIVATION AMD OXIDATIVE STRESS IN RATS WITH ALCOHOLIC HEPATITIS. ADVISOR : ASSOC. PROF. DUANGPORN THONG-NGAM, M.D., CO-ADVISOR : ASSOC. PROF. ONANONG KULAPUTANA, M.D., Ph.D., 109 pp.

Alcohol oxidation generates toxic metabolites and induces oxidative stress which contributes to the pathogenesis of alcoholic liver disease. Curcumin, the active ingredient of *Curcuma longa* Linn., is a potent antioxidant and anti-inflammation. The present study determined the possible mechanism that curcumin could attenuate liver injury induced by alcohol in rats. Female Sprague-Dawley rats were divided into four groups. Control group was fed distilled water. Alcohol group was fed 50% alcohol (7.5 g/kg BW day). Treatment groups were fed curcumin dissolved in 50% alcohol (7.5 g/kg BW day) at a dose of 400 mg/kg BW a day and 1,200 mg/kg BW a day, respectively. Alcohol or curcumin was treated via an intragastric tube for 4 weeks. Rats were sacrificed and liver samples were collected at the end of the study. The liver histopathology in alcohol group revealed mild to moderate steatosis, and mild necroinflammation. Level of hepatic malondialdehyde (MDA), hepatocyte apoptosis and NF-κB activation increased significantly when compared with control group. Curcumin treatments resulted in improving liver pathology, decreasing the elevation of hepatic MDA and inhibiting NF-κB activation. The 400 mg/kg BW of curcumin treatment revealed only a trend of decreased hepatocyte apoptosis. However, the results of superoxide dismutase activity and PPARγ protein expression showed no difference among the groups. In conclusion, curcumin could attenuate liver injury induced by alcohol through the reduction of oxidative stress and inhibition of NF-κB activation. In addition, curcumin might have a trend to decrease hepatocyte apoptosis. PPARγ protein expression may not change in early stage of alcohol-induced liver injury.

Field of Study : Physiology ..... Student's Signature Suchittra .....

Academic Year : 2008 ..... Advisor's Signature Duangporn Thong-ngam .....

Co-Advisor's Signature Onanong Kulaputana

ACKNOWLEDGEMENTS

I would like to express my sincere gratitude to my advisor, Associate Professor Duangporn Thong-Ngam and my co-advisor, Associate Professor Onanong Kulaputana for their excellent instruction, guidance, encouragement, and constructive criticism which enable me to carry out my study successfully.

I am deeply beholden to Assistant Professor Naruemon Wisedopas for histopathological examination. Grateful acknowledgement is also expressed to Associate Professor Suthiluk Pathumraj for supporting chemical and equipments.

I would like to thank Mrs. Doungsamon Suyasunanont for nutrition ingredient of rat diet. I extend my sincere thanks to Associate Professor Kanitha Patarakul and Dr. Amornpun Sereemaspun for their suggestions and the facilities used in Western blot analysis.

I also want to thank Mr. Preecha Ruangvejvorachai for facilities in studying immunohistochemistry technique and all the staffs of the Department of Physiology, Faculty of Medicine, Chulalongkorn University for their technical help in this thesis.

Furthermore, my grateful is extended to members of the thesis committee for their valuable comments and the correction of this thesis.

Finally, I am thankful to my family and my friends for their loves and supports during this educational experience.

This study had a financial support from The 90th Anniversary of Chulalongkorn University Fund (Ratchada phiseksomphot Endowment Fund) and Grant of Ratchada phiseksomphot, Faculty of Medicine, Chulalongkorn University, Bangkok, Thailand.

CONTENTS Page

CONTENTS

Page

LIST OF TABLES

LIST OF FIGURES

LIST OF FIGURES

LIST OF ABBREVIATIONS

ADH	Alcohol dehydrogenase
ALD	Alcoholic liver disease
ALDH	Aldehyde dehydrogenase
CCl_4	Carbon tetrachloride
CYP2E1	Cytochrome P450 2E1
DAB	3,3' diaminobenzidine
G3P	Glycerol-3-phosphate
HCC	Hepatocellular carcinoma
4-HNE	4-Hydroxy nonenal
H_2O_2	Hydrogen peroxide
HSC	Hepatic stellate cell
IKK	IκB-kinase
IL-12	Interleukin-12
iNOS	Inducible nitric oxide synthase
MCP-1	Monocyte chemotactic protein-1
MDA	Malondialdehyde
MESO	Ethanol oxidation system
NBT	Nitroblue tetrazolium
NF-κB	Nuclear factor-kappa B
O_2^-	Superoxide radical
OH^-	Hydroxyl radical
PAGE	Polyacrylamide gel electrophoresis
PBS	Phosphate buffer saline
PPARγ	Peroxisome proliferators-activated receptor gamma
PPRE	PPAR response element
PVDF	Polyvinylidene difluoride
ROS	Reactive oxygen species
SD	Standard deviation
SMA	Smooth muscle actin

SOD	Superoxide dismutase
TAG	Triacylglycerol
TdT	Terminal deoxynucleotidyl transferase
TNF-α	Tumor necrosis factor-alpha
TUNEL	TdT-mediated X-dUTP nick end labeling

CHAPTER I

INTRODUCTION

Background and Rationale

Alcoholic liver disease (ALD) represents a spectrum of clinical illness and morphological changes that range from fatty liver to hepatic inflammation and necrosis (alcoholic hepatitis) to progressive fibrosis (alcoholic cirrhosis) (Tome and Lucey, 2004). Recent data showed that the mortality rate for ALD was 14.3 per 100,000 population in France (Pageaux et al., 2003) and 7.9 per 100,000 in the United States (Roizen et al., 1999). Furthermore, sustained excessive alcohol intake favors the progression of other liver diseases, such as virus-related chronic hepatitis, also increasing the risk of hepatocellular carcinoma (HCC) (Bellentani et al., 1994, Safdar and Schiff, 2004).

Many of the metabolic and toxic effects of alcohol in the liver have been associated with its metabolism because it generates toxic metabolites and induces a state of oxidative stress. Importantly, chronic alcohol consumption, cytochrome P450 2E1 (CYP2E1) oxidizes ethanol to generate many toxic products, such as acetaldehyde, 1-hydroxyethyl radical, and other reactive oxygen species (ROS), such as superoxide radical (O_2^-), hydrogen peroxide (H_2O_2), and hydroxyl radical (OH^-); as well as lipid peroxidation-end products malondialdehyde (MDA) and 4-hydroxy nonenal (4-HNE) (Das and Vasudevan, 2007). Jin and co-worker observed the pathological changes and investigated the correlation on of hepatocyte apoptosis with CYP2E1 expression and oxygen free radical in rats with ALD. They found that the level of MDA in serum had a positive correlation with hepatocyte apoptosis index. In addition, the activity of superoxide dismutase (SOD) in serum had a negative correlation with apoptosis index in ALD rats, and there was negative correlation between MDA and SOD (Jin et al., 2007).

In addition, oxidative stress can activate nuclear factor-kappa B (NF-κB) transcription factor that is a key regulator of genes involving in inflammation (Pahl, 1999). Numerous target genes have been implicated in the pathogenesis of ALD, including tumor necrosis factor-alpha (TNF-α), interleukin-12 (IL-12), monocyte chemotactic protein-1 (MCP-1), macrophage inflammatory protein-2 (MIP-2), inducible nitric oxide

synthase (iNOS), and cyclooxygenase-2 (Nanji et al., 1994, 1995, 1997, 1999). All these studies indicated the significant role of NF-κB on pathogenesis of ALD.

More recently, rats with alcoholic liver fibrosis had a decrease of peroxisome proliferators-activated receptor gamma (PPARγ) expression (Zhao et al., 2004). As PPARγ is a family of ligand-activated nuclear transcriptional factor which regulates cell differentiation, apoptosis, lipid metabolism and inflammation, it may play an important role in the development of hepatocellular inflammation, necrosis and fibrosis in rats with alcohol consumption (Zhao et al., 2004).

Curcumin (diferuloylmethane), an anti-inflammatory and antioxidant compound, is isolated from the rhizomes of the plant *Curcuma longa* Linn. Activation of PPARγ by curcumin resulted in an inhibition of NF-κB *trans*-activating activity and increased expression of PPARγ at both the transcriptional and translational levels in activated hepatic stellate cells (HSCs) (Xu et al., 2003). Additionally curcumin has been reported to suppress the activation of NF-κB in alcohol-induced liver injury in rats (Nanji et al., 2003).

However, it remained unclear whether curcumin had any effects in alcoholic hepatitis rats. Therefore, the present study was designed to determine the effects of curcumin on inflammation and oxidative stress in alcoholic hepatitis rats.

Research Questions

Can curcumin attenuate inflammation and oxidative stress in rats with alcoholic hepatitis? If so, are these effects mediated through up-regulation of PPARγ and suppression of NF-κB activation?

Research Ojectives

1. To study the anti-inflammatory and antioxidant effects of curcumin in rats with alcoholic hepatitis.

2. To study the possible mechanism(s) that explain(s) the anti-inflammatory and antioxidant effects of curcumin in rats with alcoholic hepatitis.

Hypothesis

Curcumin has an attenuating effect on inflammation and oxidative stress by up-regulating PPARγ and suppressing NF-κB activation in rats with alcoholic hepatitis.

Expected Benefit and Application

Experimental data would give an understanding of the possible mechanisms that curcumin attenuates inflammation and oxidative stress in rats with alcohol-induced liver injury and it might be applied for treatment in patients with alcoholic liver disease.

CHAPTER II

THEORY AND LITERATURE REVIEW

The Liver

The liver is the largest internal organ, weighing approximately 1,500 g and accounting for nearly 2.5% of adult body weight. It is located in the upper right and partially in the upper left quadrants of the abdominal cavity, protected by the ribcage. The liver is enclosed in a capsule of fibrous connective tissue (Glisson's capsule); a serous covering (visceral peritoneum) surrounds the capsule, except where the liver adheres directly to the diaphragm or the other organs. In human the liver is anatomically divided by deep groves into two large lobes (the right and left lobes) and two smaller lobes (the quadrate and caudate) (Figure 2-1) (Ross et al., 2003).

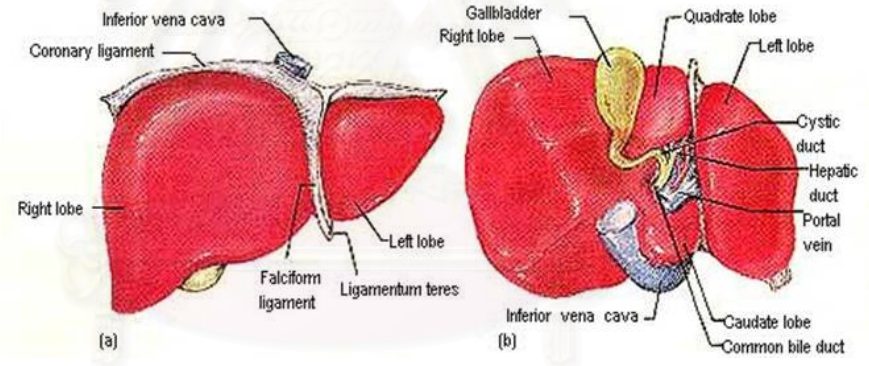

Figure 2-1. Anatomic structure of liver (a) anterior view and (b) inferior view (http://www.biomed.metu.edu.tr/courses/term_papers/bioartf-liver_kenar.htm)

1. Structural and Functional Organization of the Liver

The structural and functional organization of the liver has been described by hepatic lobule and hepatic acinus models, respectively. Hepatic lobule is defined histologically as a hexagonal region of hepatocytes which arrange around a central vein. The hepatic acinus is the smallest functional unit that is defined by the terminal branches of the portal triad. Cells in the hepatic acinus can be subdivided into zones (Figure 2-2).

Zone I called periportal area would be closest to the vessel and consequently the first to be affected by or to alter the incoming blood. Cell in zone II called midzone would be second to respond to the blood and zone III called centrilobular or periacinal area would be portal vein blood that has been previously altered by cells in both zone I and II. (Reppaport, 1956).

Five intrinsic cell types have been identified in the liver: the parenchymal cells or hepatocytes and four types of non-parenchymal cells. The non-parenchymal cells are the liver resident macrophages; the Kupffer cells; endothelial cells; the Stellate cells (also called Ito- or fat storing cells); and the pit cells (Reppaport, 1956).

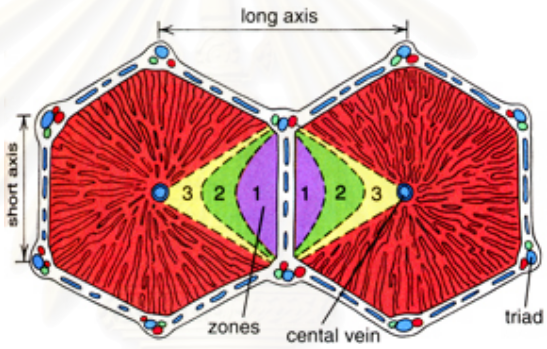

Figure 2-2. The hepatic acinus (Ross et al., 2003)

2. Blood Supply of the Liver

The liver receives blood from two sources, the hepatic artery (25%) with oxygenated blood, and the hepatic portal vein (75%) with deoxygenated blood containing newly absorbed nutrients, drugs, and possibly microbes and toxin from the gastrointestinal tract (Ross et al., 2003). Branches of both hepatic artery and hepatic portal vein carry blood into liver sinusoids. The blood drains into the central vein. Central veins drain into larger veins often called sublobular veins and these in turn drain into the hepatic veins and empty their blood into the inferior vena cava (Figure 2-3). Branches of the hepatic portal vein, hepatic artery, and bile duct typically accompany each other in their distribution through the liver. Collectively, these three structures are called a portal triad or portal tract (Tortora and Grabowski, 2000).

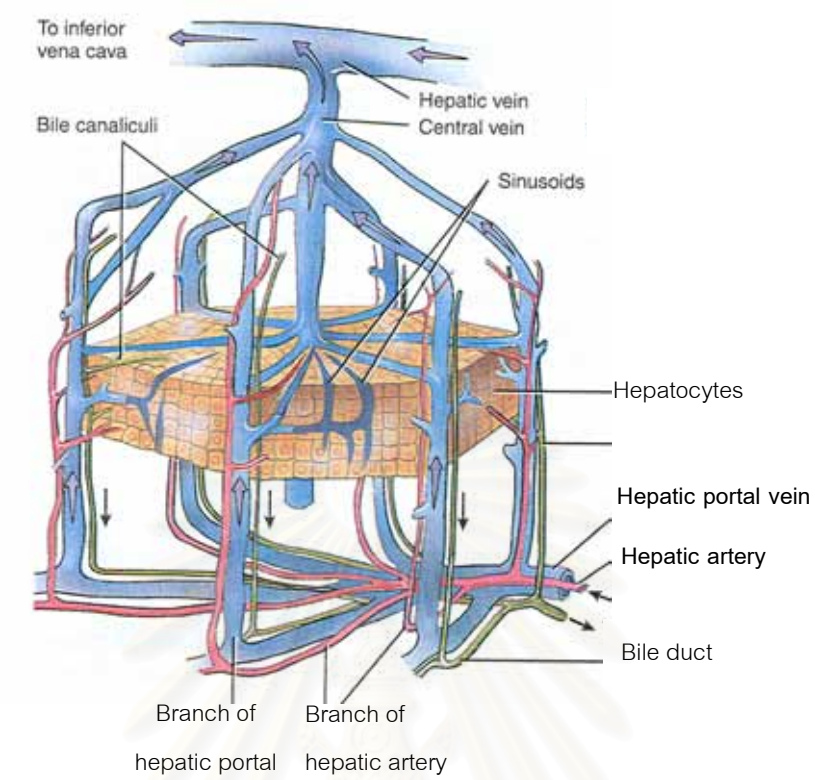

Figure 2-3. Blood supply of the liver (Tortora and Grabowski, 2000)

3. Functions of the Liver

The liver performs many vital functions (Romanes, 1986) including; first, metabolizing the products of digestion through the portal vein (principally degradation products of protein and carbohydrates); second, the storage and release of substances (principally glucose) so as to maintain a constant level in the blood; and third, the synthesis, conjugation and transformation of substances e.g. formation of protein, detoxification of poisonous substances, production of carbohydrates from protein. All of these are endocrine function which alters the composition of blood traversing the liver.

Alcoholic Liver Disease (ALD)

Alcoholic liver disease (ALD) represents a spectrum of clinical illness and morphological changes that range from fatty liver to hepatic inflammation and necrosis (alcoholic hepatitis) to progressive fibrosis (alcoholic cirrhosis) (Tome and Lucey, 2004) (Figure 2-4). Many of the metabolic and toxic effects of alcohol in the liver have been

associated with its metabolism because it generates toxic metabolites and induces a state of oxidative stress. In this review literature alcoholic hepatitis is emphasized.

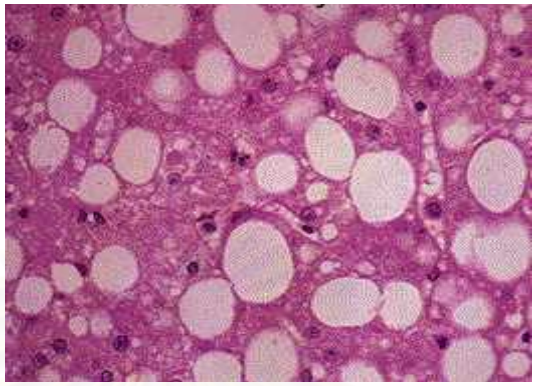

a

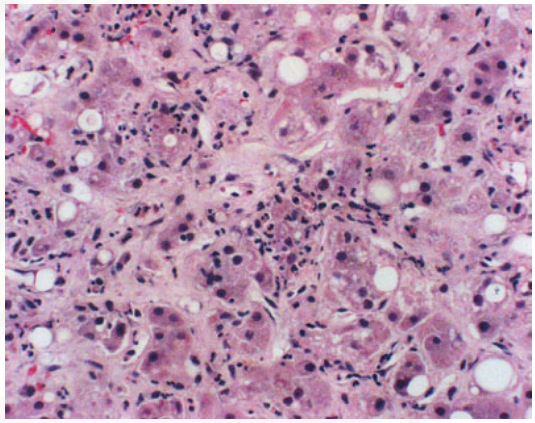

b

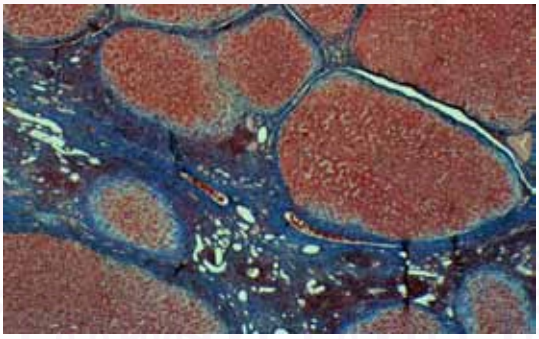

c

Figure 2-4. The pathologic spectrum of human ALD, a) fatty liver, b) alcoholic hepatitis and c) alcoholic cirrhosis

(http://www.pathology.med.umich.edu/greensonlab/etoh-fat.jpg)

(http://www.medscape.com/content/2004/00/48/89/488939/488939_fig.html)

(http://www.kumc.edu/instruction/medicine/anatomy/histoweb/path/path03.htm)

About 10-35% of alcoholics will develop alcoholic hepatitis (Ramaiah et al., 2004) Alcoholic hepatitis, also called sclerosing hyaline necrosis, is a highly characteristic histological condition. The morphological pattern in man consists of the infiltration of polymorphonuclear leukocytes, hepatocyte degeneration, and necrosis. The appearance of Mallory bodies is common, but it is not considered to be an obligatory diagnostic sign (MacSween and Burt, 1986, Hall, 1995). In biopsy steatosis is almost always present with hepatitis, or, if the biopsy is delayed, the mobilization of fat may have taken place (MacSween and Burt, 1986). Alcoholic hepatitis in most cases is a reversible condition.

Hepatitis is considered to be the most important precursor to cirrhosis, the progression of disease appearing to require one or more antecedent episodes of steatohepatitis (Diehl, 1999). The presence of alcoholic hepatitis in the initial biopsy may be of prognostic significance in the progression to cirrhosis. It is estimated that about 50% of patients with hepatitis develop cirrhosis within 10 years (Sørensen et al., 1984).

1. Alcohol Metabolism

1.1 Absorption, Distribution, and Excretion

Alcohol is absorbed from the gastrointestinal tract by simple diffusion. Because of slow absorption of alcohol in the stomach, 50-80% of absorption occurs in the duodenum and upper jejunum. The rate of absorption is delayed following a meal and increases in proportion to the alcohol concentration of the drink consumed.

Following absorption, the tissue distribution of alcohol is principally determined by blood flow and water content. Thus, in organs with a rich vasculature such as brain, lungs, and liver, alcohol levels rapidly equilibrate with the blood. Alcohol is poorly soluble in lipids which will take up only 4% of the amount of alcohol that can be dissolved in a corresponding volume of water. As a result, tissues with a high fat/water ratio attain much lower levels than organs such as the kidney, where the high water content results in urinary alcohol levels 1.3 times higher than those in blood. The low lipid solubility of alcohol also explains why, following the ingestion of the same amount of alcohol per unit weight, an obese person attains a higher level of blood alcohol than a thin person. Furthermore, the higher fat content of female body composition compared

to male has been invoked as part of the explanation of for their higher alcohol levels following the ingestion of similar amounts of alcohol per unit weight (Stewart and Day, 2006).

Over 90% of circulating alcohol is oxidatively metabolized, primarily in the liver, and excreted as carbon dioxide and water. There are three metabolic pathways of alcohol which involve the following enzymes: alcohol dehydrogenase (ADH), microsomal ethanol oxidation system (MEOS) and catalase (Figure 2-5) (Stewart and Day, 2006).

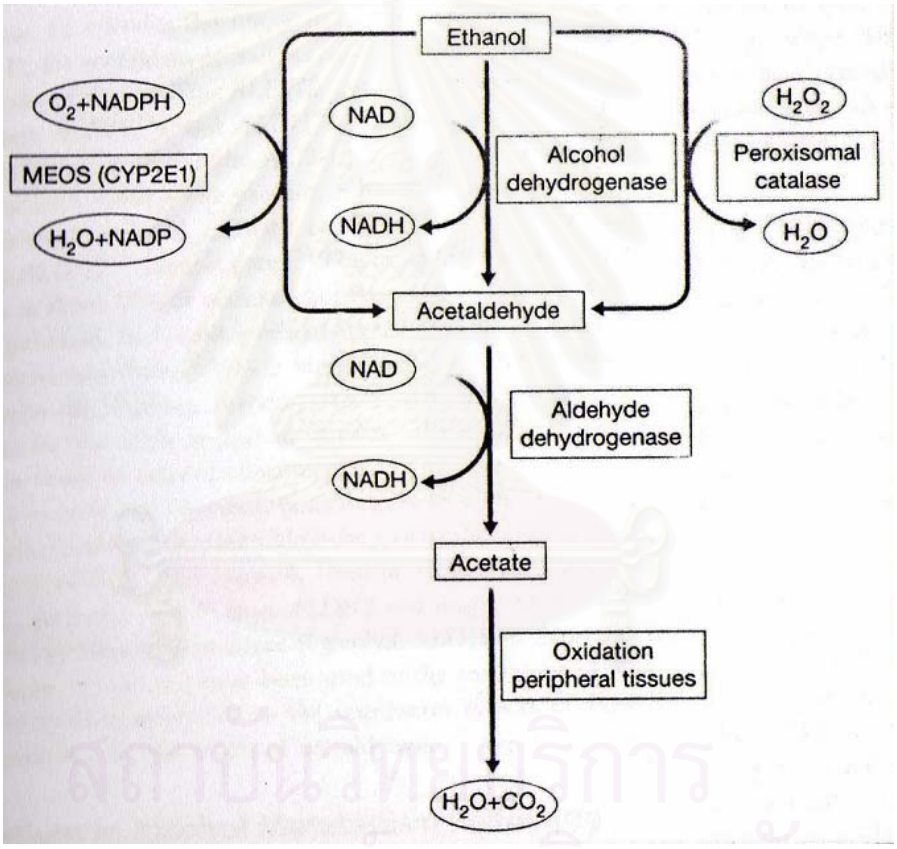

Figure 2-5. The three pathways of alcohol oxidation (Stewart and Day, 2006)

1.2 The Alcohol Dehydrogenase Pathway

Human ADH exhibits multiple isoenzymes that have been divided into four major classes which are encoded by at least seven different gene loci, *ADH1*to *ADH7*, encoding the α-, β-, γ-, π-, χ-, σ-, μ-subunits respectively. The liver contains the

highest levels of class I activity, while class III activity is present equally in all tissues. In humans, the class II isoenzyme has been found only in the liver while the class IV is present only in the stomach (Moreno and Pares, 1991). The overall K_m of liver ADH activity is 1 mmol (4mg/100 ml).

The ADHs catalyze the oxidation of alcohol to acetaldehyde. In this reaction a hydride ion is transferred from ethanol to NAD^+ which is converted to its reduced form (NADH) (Das and Vasudevan, 2007).

$$CH_3CH_2OH + NAD^+ \longrightarrow CH_3CHO + NADH + H^+$$

The resulting increase in the ratio of $NADH/NAD^+$, which is further increased by acetaldehyde oxidation, is partly responsible for the metabolic imbalances that occur following alcohol ingestion and has been considered to play a major role in the initial pathogenesis of alcohol-induced fatty liver.

1.3 The Microsomal Ethanol Oxidation System Pathway

In addition to ADH, alcohol is metabolized by the MEOS, an accessory pathway that involves a specific alcohol-inducible form of CYP2E1 (Lieber, 1999). The enzyme is located on the endoplasmic reticulum. It present in greater amounts in perivenular than periportal hepatocytes and catalyze the following reaction:

$$CH_3CH_2OH + NADPH + H^+ + O_2 \longrightarrow CH_3CHO + NADP^+ + 2HO_2$$

Its K_m for alcohol is 50-80 mg/100 ml so it appears to play an important role at high blood alcohol levels or following chronic alcohol abuse (Stewart and Day, 2006).

1.4 The Catalase Pathway

The third pathway for alcohol oxidation is catalyzed by the enzyme catalase. This enzyme is located in the peroxisomes of most tissues and requires the presence of hydrogen peroxide.

$$CH_3CH_2OH + H_2O_2 \longrightarrow CH_3CHO + 2HO_2$$

The reaction is limited by the availability of hydrogen peroxide which is low in normal circumstances, and suggests that the catalase pathway accounts for less than 2% of overall in vivo alcohol oxidation (Boveris et al., 1972).

1.5 Oxidation of Acetaldehyde to Acetate

Over 90% of the acetaldehyde formed from alcohol oxidation is further oxidized in the liver to acetate by aldehyde dehydrogenase (ALDH). ALDH, like ADH, uses NAD^+ as a cofactor and further increases the NADH/ NAD^+ (Das and Vasudevan, 2007).

$$CH_3CHO + NAD^+ \longrightarrow CH_3COOH + NADH + H^+$$

2. Alcohol Induced Liver Injury

2.1 The Metabolism of Alcohol on Fatty Change

The accumulation of triacylglycerol (TAG), synthesized via the sequential esterification of glycerol-3-phosphate (G3P) within the liver, is an early and reversible effect of alcohol consumption in humans and animal models of ALD. Hepatic levels of G3P are increased following alcohol consumption secondary to an increase in NADH/NAD^+ ratio in the liver that drives the equilibrium of the reaction to the right.

$$\text{Dihydroxyacetone P} + NADH + H^+ \longrightarrow \text{Glycerol-3-phosphate} + NAD^+$$

A consequence of increasing concentrations of G3P is enhanced rates of esterification of fatty acids that promote fatty liver. Interestingly, alcohol increases the metabolization of fatty acids by up-regulation of lipogenic enzymes, such as hepatic L-α-glycerophosphate acyltransferase or fatty acid synthesis (Brenner and Sigmund, 2004). Another factor contributing to inhibition of fatty acid oxidation in mitochondria is the increase in NADH generated by alcohol oxidation. Moreover, inhibition of lipoprotein export occurs possibly via formation of acetaldehyde protein adducts with tubulin (a protein responsible for intracellular vesicle transport), thus promoting steatosis or fatty liver (Brenner and Sigmund, 2004).

2.2 Oxidative Stress and Inflammatory Response

Oxidative stress plays a pivotal role in the development of ALD. The most important enzyme CYP2E1 not only generates acetaldehyde, but also other ROS, including hydroxyethyl radical, H_2O_2, HO^- and O^-_2 (Brenner and Sigmund, 2004). These free radicals can promote toxicity by protein oxidation, oxidative damage to the DNA, and disturbing cell membranes via lipid peroxidation and production of reactive lipid aldehydes, such as MDA and HNE (Gate et al., 1999). An increase in mitochondrial membrane permeability allows the leakage of apoptosis-inducing factors (predominately cytochrome C) into the cytosol, where they can activate caspases and initiate the apoptic cascade in hepatocytes (Natori et al., 2001). In addition, oxidative stress can mediate liver injury through cell signaling. For example, activation of transcription factors such as NF-κB which play a critical role in the production of inflammatory cytokines such as TNF-α, IL-1 and IL-6 (Pahl, 1999).

In fact, alcohol metabolites, such as acetaldehyde and MDA, which are resulted from lipid peroxidation, interact through a covalent binding with the reactive lysine residues of proteins located on the membrane of hepatocytes. This leads to the formation of stable protein adducts which have been shown to be immunogenic (neo-antigens). These neo-antigens may induce an immune reaction with antibody production or T-cell activation or both resulting in tissue damage (Gramenzi et al., 2006).

Oxidative Stress

Oxidative stress has been defined as a disturbance of the balance between antioxidants and prooxidants (free radicals and other reactive oxygen and nitrogen species) with increased levels of pro-oxidants leading to potential damage (Halliwell, 1997, Sies, 1997, Betteridge, 2000). This imbalance can be an effect of depletion of endogenous antioxidants, low dietary intake of antioxidants and/or increased formation of free radicals and other reactive species.

1. Free Radicals and Other Reactive Species

Free radicals can be defined as any chemical species that contains unpaired electrons. Unpaired electrons increase the chemical reactivity of an atom or molecule.

Common examples of free radicals OH, O_2^-, transition metals such as iron and copper, nitric oxide, and peroxynitrite.

The hydroxyl radical, the most potent oxidant known, has an extremely short half-life, reacting at the site of its formation through its ability to attack most biological molecules resulting in the propagation of free radical chain reactions. Superoxide is formed when oxygen accepts an electron and is not in itself particularly reactive. It can act as a weak oxidizing agent, but is much stronger as a reducing agent of iron complexes such as cytochrome C. It is likely to be more important as a source of OH^- and H_2O_2 (Betteridge, 2000).

2. Free Radicals Induced Cellular Damage

Proteins are made up of approximately 20 different building blocks called amino acids, which differ in their sensitivity to interactions with free radicals. For example, the amino acids cysteine, methionine, and histidine are especially sensitive to attack and oxidation by OH^-. Accordingly, enzymes in which these amino acids are located at positions that are critical to the enzyme's activity will become inactivated by the interaction with free radicals. Alternatively, the free radical-induced oxidation of proteins can lead to changes in the proteins three-dimensional structure as well as to fragmentation, aggregation, or cross-linking of the proteins. Finally, protein oxidation often will make the marked protein more susceptible to degradation by cellular systems responsible for eliminating damaged proteins from the cell.

Free radicals are a major source of DNA damage, causing strand breaks, removal of nucleotides, and a variety of modifications of the organic bases of the nucleotides. Although cells have developed repair mechanisms to correct naturally occurring changes in the DNA, additional or excessive changes caused by ROS or other agents can lead to permanent changes or damage to the DNA, with potentially detrimental effects for the cell.

Lipids that contain phosphate groups (i.e., phospholipids) are essential components of the membranes. Consequently, damage to the phospholipids will compromise the viability of the cells. The complete degradation (i.e., peroxidation) of lipids is a hallmark of oxidative damage. The polyunsaturated fatty acids present in the

membranes phospholipids are particularly sensitive to attack by OH^- and other oxidants. OH^- can result in the peroxidation of many polyunsaturated fatty acid molecules because the reactions involved in this process are part of a cyclic chain reaction. In addition to damaging cells by destroying membranes, lipid peroxidation can result in the formation of reactive products that themselves can react with and damage proteins and DNA (Wu and Cederbaum, 2003).

3. How is Oxidative Stress Measured?

In general terms, oxidative stress can be assessed by measurement of reaction products of oxidative damage, for example, lipid peroxidation, DNA oxidation, and protein oxidation.

MDA, the secondary products derived from peroxidation of polyunsaturated fatty acids, is a biomarker of oxidative damage to lipids. MDA is moderately reactive and it can act both as an electrophile and as a nucleophile. It reacts with biomolecules containing primary amino groups, such as proteins, nucleic acids and amino phospholipids (Janero, 1990). Both MDA level and antibodies to MDA-adducted protein have been demonstrated in animal model of ALD (Rouach et al., 1997, Polavarapu et al., 1998, Ronis et al., 2005). This data confirm role of oxidative stress in ALD.

Antioxidant Defense

Oxidative stress may be harmful to the liver if the defensive capacity is not able to cope with the increased free radical generation. Under normal conditions, hepatic oxidative stress is efficiently counteracted by antioxidant system. The system includes enzymatic antioxidants and non-enzymatic antioxidants. Antioxidant enzymes or “scavenging enzymes” provide the first line of defense against ROS by converting them to more reduced and more stable species. The three major scavenging enzymes are SOD, catalase, and glutathione peroxidase (Figure 2-6). A second line of defense is provided by non-enzymatic or exogenous antioxidants obtained primarily as nutrients or nutritional supplements such as carotenoids, reduced glutathione, vitamin E, and vitamin C (Gate, 1999, Chaudiere, 1999).

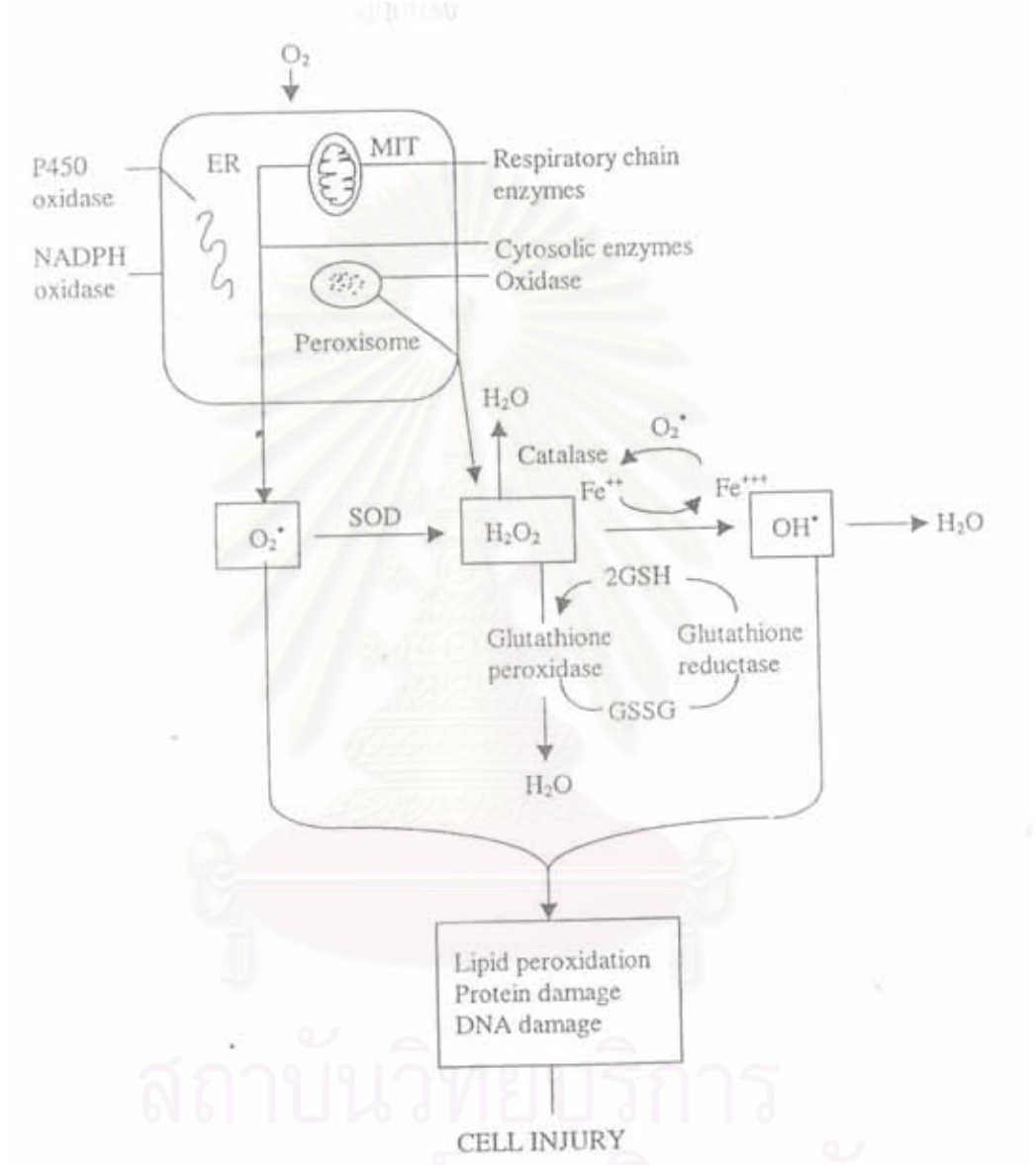

Figure 2-6. Antioxidant system to deal with the production of ROS (Halliwell et al., 1984)

Superoxide Dismutase (SOD)

SOD converts O_2^- into a less toxic product, H_2O_2 and H_2O. This enzyme is the first line in cell defense against oxidative stress (Gate, 1999).

$$2O_2^- + 2H^+ \longrightarrow H_2O_2 + O_2$$

There are three types of SOD, depending on the metal ion bound to its active site. Copper-and zinc-containing SOD (CuZn-SOD) is a highly stable enzyme found primarily in the cytosolic compartment of eukaryotic cells such as yeast, plant and animals. Manganese-containing SOD (Mn-SOD) is present in the mitochondrial matrix. Bacteria contain a third type of SOD, which requires iron as a prosthetic group (Fe-SOD) (Ji and Hollander, 2000). SOD could be inactivate by free radicals generated during alcohol metabolism and a decrease in SOD activity has been observed in rats with alcohol administration (Polavarapu et al., 1998, Ozaras et al., 2003, Uzun et al., 2005, Jin et al., 2007, Faremi et al., 2008)

Nuclear Factor-kappa B (NF-κB)

NF-κB is a transcription factor that plays a key role in regulating the host immune and inflammation. The mammalian NF-κB protein family members, including p50, p52, c-Rel, RelA (p65), and RelB, share an N-terminal domain called the Rel homology (RH) domain. The RH domain contains sequences responsible for dimerization, DNA binding nuclear localization and IκB binding. The NF-κB commonly refers to a p50-RelA heterodimer, is one of the most avidly forming dimmers and is the major Rel complex in most cells (Figure 2-7) (Gilmore, 1999).

Regulation of NF-κB

In most cells, NF-κB is present as a latent, inactive, IκB-bound complex in the cytoplasm. Most agents that induce IκB degradation, including TNF-□, IL-1, LPS, oxidative stress, accomplish complicate degradation via an IκB-kinase (IKK) enzyme. The IKK is an unusual kinase which contains two related kinases, IKK-□ and IKK-β, that are active as a dimer. Activation of IKK leads to the phosphorylation of two specific serines near the N terminus of IκB-□, which targets IκB-□ for ubiquitination and

degradation by the proteosome. NF-κB rapidly enters the nucleus and activates gene expression. One of the target genes activated by NF-κB is IκB-□ (Figure 2-8) (Gilmore, 1999, Pahl, 1999).

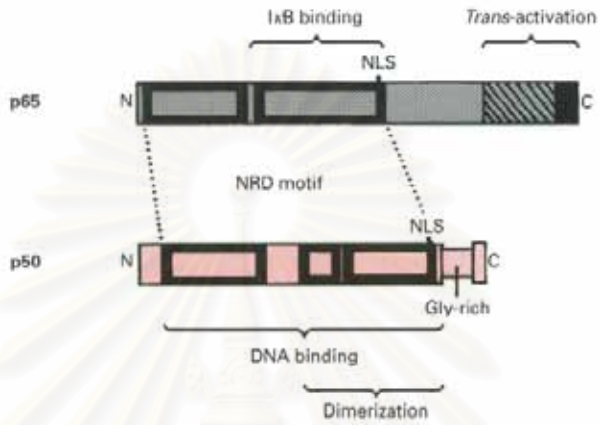

Figure 2-7. Structure of p65 and p50 NF-κB subunits (Grimm and Baeuerle, 1993)

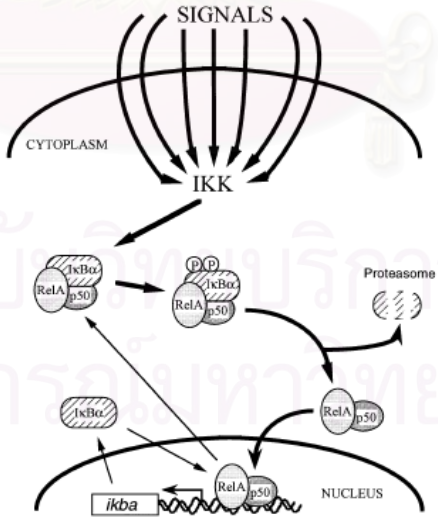

Figure 2-8. Regulation of NF-κB (Gilmore, 1999)

The NF-κB activation promotes the expression of over 150 target genes. The majority of proteins that are encoded by NF-κB participate in the host immune response. For example, cytokines and chemokines, as well as receptors required for immune recognition, such as MHC molecules, proteins involved in antigen presentation and receptors required for neutrophil adhesion and transmigration across blood vessel wall (Pahl, 1999). Some experiments have been shown role of NF-κB activation in pathogenesis of ALD (Nanji et al., 1999, 2003, Jokelainen, 2001, Yuan, 2006).

Peroxisome Proliferator-Activated Receptor γ (PPARγ)

Peroxisome proliferator-activated receptors (PPARs) are members of the nuclear hormone receptors family. PPARs are a family of 3 ligand-activated transcription factors: PPARα (NR1C1), PPARβ/δ (NUC1; NR1C2), and PPARγ (NR1C3). PPARγ has a characteristic modular structure consisting of several functional domains. The AF-1 is a constitutively activated ligand-independent transactivation function. The C domain contains the DBD targeting the receptor to specific hormone response elements on DNA. The D domain constitutes a cofactor-docking region. The carboxy-terminal portion (E) encompasses the LBD, a dimerization interface and the ligand-dependent activation domain AF-2 (Figure 2-9) (Debril et al., 2001).

Figure 2-9. PPARγ functional domains (Debril et al., 2001)

1. PPARγ Ligands

PPARγ is bound and activated by several naturally occurring compounds, such as 15-PGJ_2, docosahexaenoic acid, linoleic acid, as well as by synthetic molecules, such as thiazolidinediones. Upon binding these ligands, PPARγ undergoes a conformational change, stabilizing its interaction with the RXR. This allows the

recruitment of a set of cofactors, and stimulates the transcription of target genes (Debril et al., 2001).

2. Molecular Mechanism of PPARγ Action

In the inactivated state, PPARγ is considered complexes bound with co-repressor proteins. Upon ligand activation, PPARγ dissociates from co-repressors and recruit co-activators. Then the activated PPARγ–RXR heterodimer complex binds to DNA sequences called PPAR response elements (PPRE) in target genes initiation their transcription (Figure 2-10) (Moraes et al., 2006). PPARγ plays important roles in the regulation of lipid metabolism, stimulation of adipocyte differentiation and insulin action, apoptosis pathway and inflammatory processes.

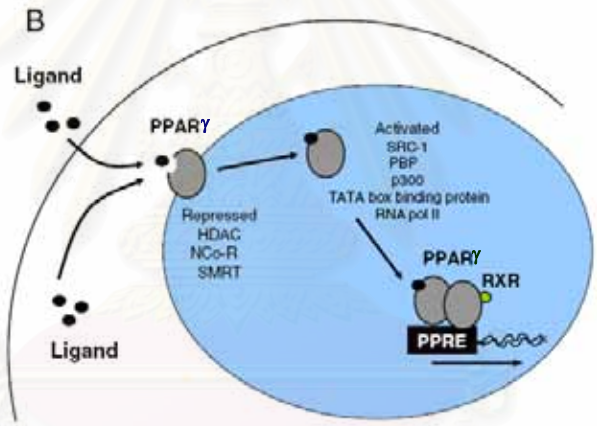

Figure 2-10. Regulation of PPARγ (Moraes et al., 2006)

3. Role of PPARγ in Inflammation

There are many of experimental data that indicated role of PPARγ in inflammation. *In vitro* study showed that PPARγ ligands inhibited the induction of iNOS, MMP-9, and scavenger receptor A gene transcription. PPARγ activation inhibited the transcriptional activity of cytokine induced pro-inflammatory transcription factors AP-1, NF-κB, and STAT1 transcription factors (Ricote et al., 1998). Furthermore, PPARγ activators decreased LPS-induced expression of TNF-α in neonatal rat cardiac myocytes (Takano et al., 2000). *In vivo* study, PPARγ ligands attenuated the inflammatory

response in sepsis through regulation of the NF-κB and AP-1 pathways (Zingarelli et al., 2003). Interestingly, PPARγ activation inhibited TNF-α in a cute and chronic liver injury induced by ethanol and lipopolysaccharide (Enomoto et al., 2003, Ohata et al., 2004). Also, the expression of PPARγ in rat liver correlated negatively with the degree of its inflammation, necrosis and fibrosis in alcohol induced liver fibrosis rats (Zhao et al., 2004).

Alpha-Smooth Muscle Actin (α-SMA)

In normal liver, HSC are non-parenchymal, quiescent cells that have three main physiological functions as vitamin A storage, production of extracellular matrix protein in the space of Disse and a role in the regulation of the sinusoidal microcirculatory flow (Carpino et al., 2005). However, in response to liver injury HSC undergo an "activation" process characterized by proliferation and myofibroblastic transformation. The activation of HSC shows an intense cytoplasmic α-SMA immunoreactivity. α-SMA is an actin isoform and a specific marker for smooth muscle cell differentiation (Skalli et al., 1986). Therefore, α-SMA expression has been used to identify activated HSC that show a myofibroblastic phenotype (Nouchi et al., 1991). Moreover, many studies showed that HSC activation decreased PPARγ expression (Miyahara et al., 2000, Zhao et al., 2004).

Curcumin (Diferuloylmethane)

Curcumin (diferuloylmethane), the natural yellow pigment in turmeric, is isolated from the rhizomes of the plant *Curcuma longa* Linn (Figure 2-11). It constitutes about 2-8% of the composition of turmeric (Sharma, 2005). The structure of curcumin is depicted in Figure 2-12.

Figure 2-11. *Curcuma longa* Linn

(http://www.ics.trieste.it/MAPs/MedicinalPlants_Plant.aspx?id=605)

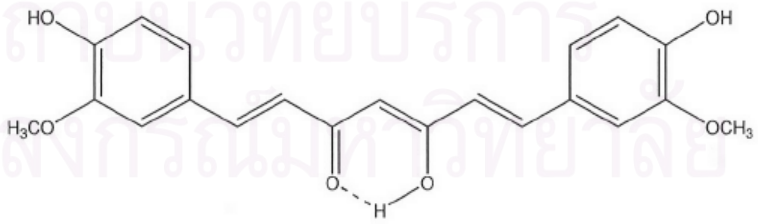

Figure 2-12. Chemical structure of curcumin (Joe, 2004)

1. Pharmacokinetic Study and Safety

Curcumin is dissolved in organic solvents such as dimethylsulfoxide, oil, alcohol, and petroleum agents. In animals, the previous study demonstrated that curcumin is poorly absorbed and rapidly metabolized in Sprague-Dawley rats (Wahltrom and Blennow, 1978, Ravindranath and Chandrasekhara, 1980 and 1982, Pan et al., 1999). Administrating curcumin orally was made by Wahlström and Blennow (Wahltrom and Blennow, 1978). They demonstrated that this compound in a dose of 1 to 5 g/kg BW given to rats apparently did not cause any adverse effects and it was excreted about 75% in the feces, while traces appeared in the urine. In addition, measurements of blood plasma levels and biliary excretion showed that curcumin was poorly absorbed by the gastrointestinal tract.

In 1999, Pan et al. investigated the pharmacokinetic properties of curcumin in mice. After intraperitoneal administration of curcumin (0.1 g/kg) in mice, approximately 2.25 μg/ml of curcumin appeared in the plasma within the first 15 min. To clarify the nature of the metabolites of curcumin, the plasma was analyzed by reversed-phase HPLC and two putative conjugates of curcumin were observed. To investigate the nature of these glucuronide conjugates *in vivo*, the plasma was analyzed by electrospray. Curcumin was first biotransformed to dihydrocurcumin and tetrahydrocurcumin, and that these compounds subsequently were converted to monoglucuronide conjugates (Figure 2-13). Ireson et al. studied the biotransformation of curcumin by human and rat hepatocytes and identified hexahydrocurcumin and hexahydrocurcuminol as the major metabolites of curcumin (Ireson et al., 2001). The chemical structures of dihydrocurcumin, tetrahydrocurcumin, hexahydrocurcumin, and hexahydrocurcuminol are depicted in Figure 2-13.

Curcumin has been demonstrated the safety in human and rats. Oral LD_{50} of curcumin was found to be 12.2 g/kg BW in rats (Arora et al., 1971). Human appeared to be able to tolerate high doses of curcumin without significant side-effects. A phase 1 study by Cheng et al. (Cheng et al., 2001), found no adverse effects of curcumin ingestion for 3 months of doses up to 8,000 mg/day.

2. Antioxidant Property of Curcumin

The discovery of the antioxidant properties of curcumin explains many of its wide ranging pharmacological activities. The phenolic and the methoxy groups on the benzene rings are important structural features that contribute to its antioxidant properties (Sreejayan and Rao, 1996 and 1997). Curcumin is an effective antioxidant and scavenges O_2^-, H_2O_2, and nitric oxide from activated macrophages (Joe and Lokesh, 1994). It inhibited the inducible nitric oxide synthase activity in macrophages (Brouet and Ohshima, 1995). Oral administration of 30 mg/kg BW of curcumin in rats for 10 days reduced the iron-induced hepatic damage by lowering lipid peroxidation (Reddy and Lokesh, 1996). Protection from radiation by dietary curcumin administered to mice is also attributed to the antioxidant property of curcumin. In addition, curcumin inhibited liver injury in carbon tetrachloride (CCl_4) induced hepatotoxicity in rats (Park et al., 2000). Interestingly, curcumin enhanced the activities of other antioxidants, such as SOD, catalase, and glutathione peroxidase (Reddy and Lokesh, 1994).

3. Antiinflammatory Property of Curcumin

Macrophages, when activated, generate a number of proinflammatory cytokines. The pleiotropic cytokine, TNF-α, induces the production of IL-1β, and together, they play significant roles in many acute and chronic inflammatory and autoimmune diseases. *In vitro* studies show that curcumin, at 5 μM, inhibited the LPS-induced production of TNF-α and IL-1β by a human monocytic macrophage cell line (Chan, 1995). As a consequence, downstream events involving TNF-α and IL-1β are affected. For instance, TNF-α induced expression of leukocyte adhesion proteins, such as intercellular adhesion molecule-1 and vascular cell adhesion molecule-1 (Gupta and Ghosh, 1999). Importantly, curcumin suppressed induction of NF-κB-dependent genes in alcohol-induced liver injury.

All these studies showed that curcumin is an antiinflammatory substance because it can inhibit the activation of the major transcription factor NF-κB. This transcription factors required for the expression of many genes linked with host immune response, such as TNF-α, IL-1β, iNOS, IL-12, MCP-1, MIP-2, and COX-2. Singh and Aggarwal observed that curcumin inhibited NF-κB activation pathway after the

convergence of various stimuli mediated by protein tyrosine kinase, protein kinase, and ubiquitin conjugation enzymes (Singh and Aggarwal, 1995). Specifically curcumin inhibited the step before the phosphorylation and subsequent release of IκB complexed to NF-κB (Singh and Aggarwal, 1995). Curcumin prevented phosphorylation of IκB by inhibiting the activity of IKK (Jobin et al., 1999, plummer et al., 1999). Brennan and O'Neill (1998) found that curcumin inhibited NF-κB by interfering with IκBα degradation and reacts with p50 in the NF-κB complex.

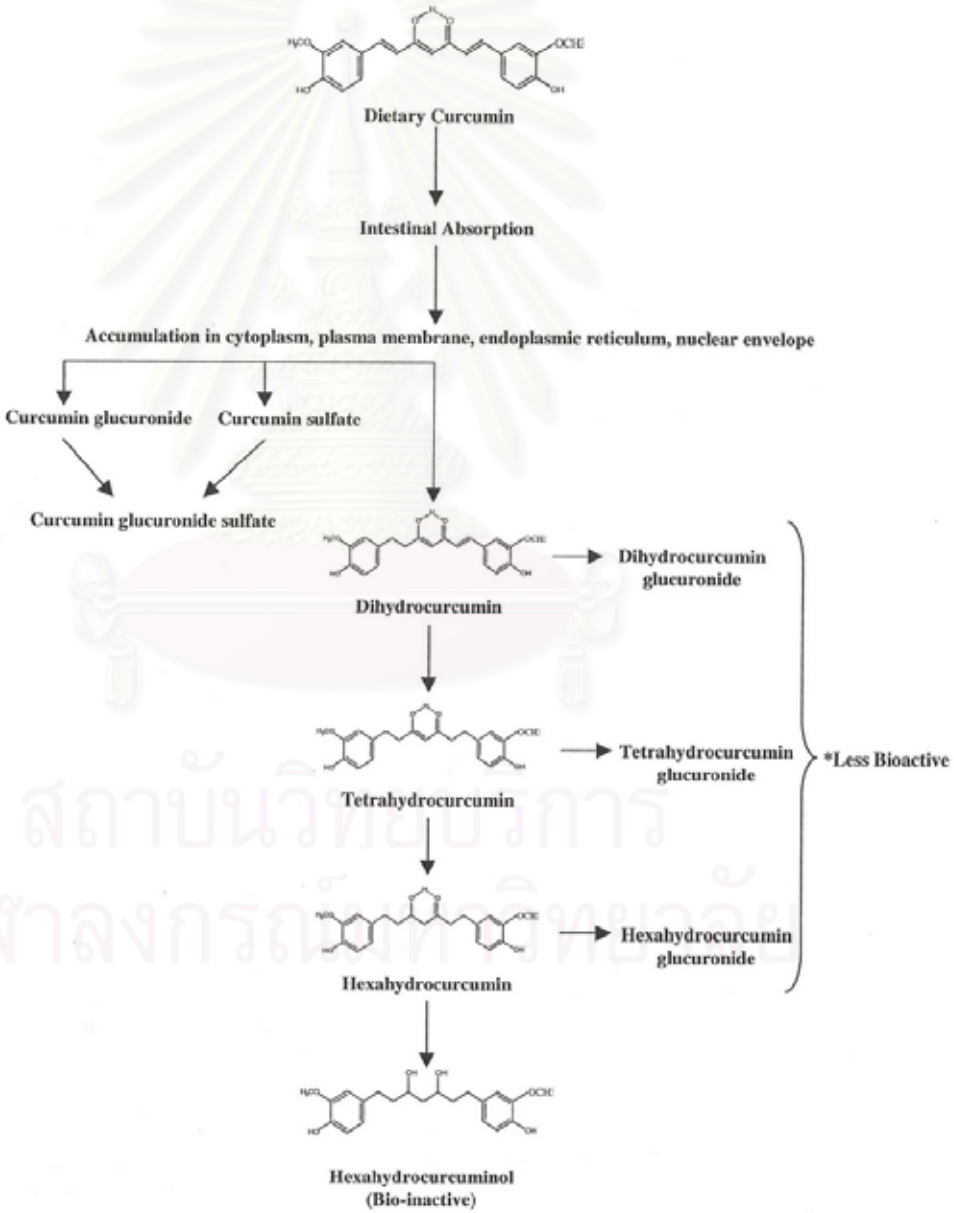

Figure 2-13. Absorption and metabolism of curcumin (Joe, 2004)

Animal Models of Alcohol-Induced Liver Injury

1. The Liquid Diet Model

The simplest method for providing alcohol chronically is through the drinking water. However, factors such as the animals' aversion to alcohol, dehydration resulting from insufficient fluid intake, nutritional imbalance, and low blood alcohol concentrations resulting from low consumption make this method unsuitable for many types of studies. To address these issues, DeCarli and Lieber developed a liquid diet that was offered to rats as the only source of food and water (Table 2-1) (Lieber and Decarli, 1989). Although rats generally dislike alcohol, when given a choice of consuming the alcohol-containing diet or starving, they choose the former and consume 14-18 g of alcohol per kilogram bodyweight, usually over a period of 4-6 weeks. This treatment regimen induces the earliest form of liver damage (i.e., fatty liver) and damage to a key type of liver cell, which can be detected with an electron microscope.

Table 2-1. Energy distribution of ethanol and control diets (calories) (Lieber and Decarli, 1989).

Diet	Alcohol	Control
Alcohol	35.5	0
Diet		
Fat	35	35
Carbohydrate	11.5	47
Protein	18	18

2. The Intragastric Model

Tsukamoto and co-workers develop the intragastric model for inducing liver damage in rats, based on the hypothesis that excessive alcohol intake and sustained high blood alcohol levels were necessary for induction of progressive liver injury. In this model, ethanol (an average of 12-15 g/kg/day in rats) and liquid diet (25% of calories as protein, 25% as fat, and 18% as carbohydrate) were fed through a permanent indwelling intragastric catheter for 30 to 120 days. This model develops fatty liver, localized necrosis and inflammation in 30 days and mild portal fibrosis in 85 days. Although there

are distinct advantages of enteral alcohol feeding, especially the ability to deliver controlled high doses of ethanol to increase pathology, disadvantages of intragastric ethanol feeding including the need for surgical manipulation, significant animal husbandry, and the relative cost of model compared to ad libitum feeding (Tsukamoto et al., 1986).

3. Enomoto and Co-Worker Model

More recently, Enomoto and colleagues reported a new model in which female Wistar rats were fed ad libitum a liquid diet. In this diet 35% of calories were from corn oil, 47% from maltose-dextrin, and 18% as protein. Rats received 5 g/kg alcohol by an 18-gauge oral biomedical device every 24 hours. After 4 weeks, this treatment induced fat accumulation, inflammation, and necrosis in the liver (Enomoto et al., 1999).

The scientific evidence has showed that gender difference associate alcohol-induced liver injury (Iimuro et al., 1997, Kono et al., 2000, Yin et al., 2000). Administration of alcohol to female rats resulted in more hepatic steatosis, inflammation and necrosis compared to male rats, despite equal alcohol intake, metabolism and excretion (Iimuro et al., 1997). Plasma endotoxin levels were also significantly higher in female rats than in male rats (Iimuro et al., 1997). In another study demonstrated that alcohol ingestion resulted in a stronger activation of the inflammation-associated transcription factor NF-κB and higher expression of CD14 and TNF-α in livers of female rats compared to male rats (Kono et al., 2000). Lowering estrogen levels, by subjecting female rats to ovariectomy, resulted in a significant reduction of alcohol-induced liver injury (Yin et al., 2000). Taken together, these results indicate that female is more susceptible to alcohol-induced liver injury.

4. Preliminary Study of ALD Model in This Thesis

As described above, there is no animal model that fed only alcohol to induce liver injury. Diet, sex, duration and dose of alcohol feeding influence to alcohol-induced liver injury. For our preliminary study, the oral feeding rat model for ALD was used. Male and female Sprague-Dawley rats were fed orally with various doses of alcohol feeding and duration (Table 2-2). Histopathological changes were evaluated by pathologist who

is blinded to the experiment. The comparative histopathology was shown in Table 2-2 and examples of liver histopathology were shown in Figure 2-14.

Group 1, 2 and 3 appeared normal histological features. Group 4 showed fatty change and mild necroinflammation at week 4 but no necroinflammation was found at 8 weeks. Only mild fatty change revealed in group 4 at week 8. Moreover, only custom diet (group 5) did not affect liver histopathology. This data supported that role of dietary polyunsaturated fatty acid may potentiate alcohol-induced liver injury. Thus, in our thesis, female Sprague-Dawley rats fed with alcohol 7.5 g/kg BW + custom-made diet (group 4 at 4 weeks) were used to study role of curcumin on changes of PPARγ expression, NF-κB activation and oxidative stress in rats with alcoholic hepatitis (more detail see Appendix A).

Table 2-2. The histopathological changes in rats

Group	Sex	Histopathological changes in rat liver				
		4 weeks	8 weeks	10 weeks	14 weeks	24 weeks
1) Alcohol 5 g/kg BW	Male	-	Normal	-	-	Normal
	Female	-	Normal	-	-	-
2) Alcohol 7 g/kg BW	Male	-	-	Normal	Normal	-
	Female	-	-	-	-	Normal
3) Alcohol 7.5 g/kg BW	Male	Normal	Normal	-	-	-
	Female	Normal	Normal	-	-	-
4) Alcohol 7.5 g/kg BW +Custom diet	Female	Fatty change and mild necroinflammation	Fatty change	-	-	-
5) Custom diet	Female	Normal	Normal	-	-	-

Note: Custom-made diet contained 35% of energy from fat, 18% from protein and 47% from carbohydrate (Enomoto et al., 1999) and ingredients of diet were showed in Appendix B.

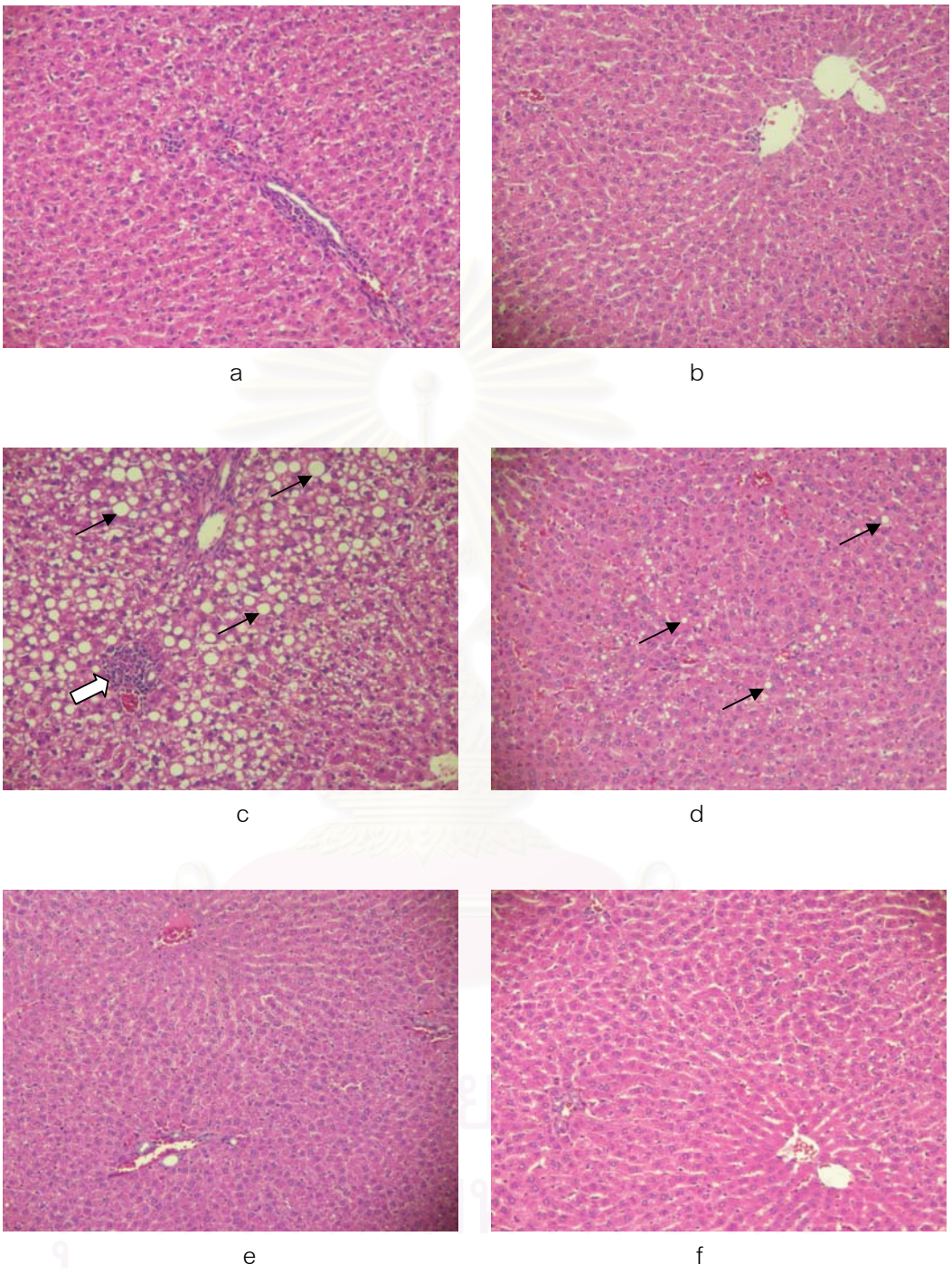

Figure 2-14. Hematoxylin-eosin stained liver sections (x400), a) group 1 (male at 24 weeks), b) group 2 (female at 24 weeks), c) group 4 (female at 4 weeks) showed fatty change (small arrows) and mild necroinflammation (block arrow), d) group 4 (female at 8 weeks) showed only fatty change, e) group 5 (female at 4 weeks) and f) group 5 (female at 8 weeks)

CHAPTER III

MATERIALS AND METHODS

This research design was animal experimental design to study role of curcumin on changes of PPARγ expression, NF-κB activation and oxidative stress in rats with alcoholic hepatitis. Female Sprague-Dawley rats were fed with alcohol to induce alcoholic hepatitis and treated with curcumin for 4 weeks. After the end of experiment, liver samples were analyzed for histopathology, apoptosis, level of hepatic MDA and SOD activity, NF-κB expression, PPARγ expression and α-SMA expression.

.

Reagents

Acetic acid (Merck, Germany)

Acrylamide (Bio Basic Ing, CA)

β-Actin antibody (sc-47778, Santa Cruz Biotechnology Inc.,USA)

95% Alcohol (Merck, Germany)

Ammonium persulfate (Bio Basic Ing, CA)

ApopTag® plus peroxidase *In Situ* apoptosis detection kit (Chemicon, USA)

Bis-acrylamide (Bio Basic Ing, CA)

Bovine serum albumin (Bio Basic Ing, CA)

Bromophenol blue (Bio Basic Ing, CA)

n-Butanol (Merck, Germany)

Citric acid monohydrat (Merck, Germany)

Curcumin (Cayman Chemical Company, USA)

Developer (Kodak, USA)

Distilled water

DTT (Bio Basic Ing, CA)

ECL plus western blotting detection reagent (Amersham, USA)

EDTA (Bio Basic Ing, CA)

Eosin (C.V. Laboratories, Thailand)

Fixer (Kodak, China)

Folin ciocalteu's phenol reagent (Sigma, USA)

Formalin solution

Glycerol (Bio Basic Ing, CA)

Glycine (Research Organics, USA)

Goat anti-mouse IgG HRP (Cayman Chemical Company, USA)

Hematoxylin (C.V. Laboratories, Thailand)

30% Hydrogen peroxide (Merck, Germany)

KCl (Merck, Germany)

Lithium carbonate (Merck, Germany)

Malondialdehyde bis solution (Sigma, USA)

Medical X-Ray film blue (Agfa, Belgium)

NaH_2PO_4 H_2O (Merck, Germany)

NaCl (Merck, Germany)

Na_2CO_3 (Merck, Germany)

Na_2HPO_4 (Merck, Germany)

NaOH (Merck, Germany)

NF-κB p65 antibody (sc-109, Santa Cruz Biotechnology Inc.,USA)

Nitroblue tetrazolium (Fluka BioChemika, Switzerland)

Normal horse serum (Santa Cruz Biotechnology Inc.,USA)

Phosphate buffer saline

Phosphatase inhibitor cocktail 2 (Sigma, USA)

Polyvinylidene difluoride (PVDF) membrane (Pall, USA)

PPARγ antibody (sc-7273, Santa Cruz Biotechnology Inc.,USA)

Protease inhibotor cocktail (Sigma, USA)

Proteinase K (DAKO, USA)

Pyridine (Sigma, USA)

Riboflavin (Sigma, USA)

Skim milk power (Fluka BioChemika, Switzerland)

α-SMA antibody (Santa Cruz Biotechnology Inc.,USA)

Sodium dodecyl sulfate (SDS) (Bio Basic Ing, CA)

Super sensitive polymer-HRP detection kit (Bio Genex, CA)

TEMED (Bio Basic Ing, CA)

Thick blotting papers (Bio-Rad, USA)

Thiobarbituric acid (Sigma, USA)

Tris (Research Organics, USA)

Triton-X100 (Bio Basic Ing, CA)

Tween 20 (Bio Basic Ing, CA)

Xylene (Zenith Science CO.LTD, Thailand)

Animal Preparation

Female Sprague-Dawley rats, weighing 180-220 g, were purchased from the National Laboratory Animal Center, Mahidol University, Salaya, Nakorn Pathom. The rats were kept in a controlled temperature room at 25 ± 1^{0}C under standard conditions (12 hour light:dark) and had freely access to food and tap water. All rats were received well care in accordance with the Ethical Committee, Faculty of Medicine, Chulalongkorn University, Thailand (approval No. 12/2551).

Curcumin Preparation

Curcumin in powder form (Cayman Chemical Company, USA) was dissolved in 50% alcohol that freshly prepared for the experiment.

Experimental Protocols

All rats were fed with the custom diet which contained 35% of energy from fat, 18% from protein and 47% from carbohydrate (Enomoto et al., 1999). They were randomly divided into four experimental groups. All groups were fed distilled water, alcohol or curcumin orally via an intragastric tube twice a day for 4 weeks.

Group 1 (Control, n=8): Rats were fed distilled water (2.0 ml)

Group 2 (Alcohol, n=8): Rats were fed 50% alcohol (7.5 g/kg BW day)

Group 3 (Alcohol+curI, n=6): Rats were fed curcumin (200 mg/kg BW) dissolved in 50% alcohol (7.5 g/kg BW day) (Shapiro et al., 2006).

Group 4 (Alcohol+curII, n=7): Rats were fed curcumin (600 mg/kg BW) dissolved in 50% alcohol (7.5 g/kg BW day)

All rats were weighed weekly. At the end of the study, they were sacrificed using intraperitoneal injection of an overdose of thiopental sodium. The abdominal wall was opened and the whole liver was removed. The liver was cut into several pieces. Three small pieces were collected, frozen in liquid nitrogen, and stored at -80 ^{o}C for MDA analysis, SOD activity, PPARγ and α-SMA protein expression. The remaining of the liver was fixed in 10% formalin solution to determine histopathology, NF-κB activation and hepatic apoptosis. The study design was summarized in the diagram below (Figure 3-15).

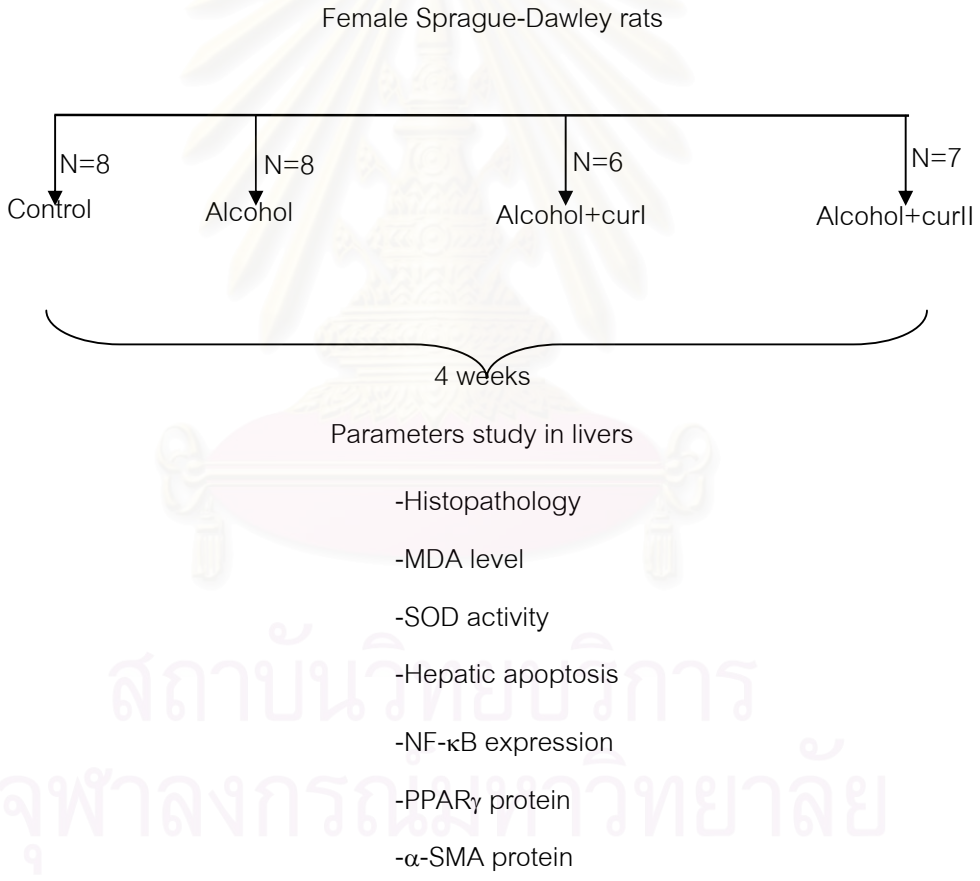

Figure 3-15. Diagram of experimental design

Data Collection

1. Histopathological Examination

Procedure

1. Liver samples were embedded in paraffin, sectioned at 5 μm and put on slides

2. The slides were deparaffinized in 3 changes of xylene for 5 minutes, hydrated in 3 changes of 95% alcohol for 5 minutes and run with tap water for 3 minutes.

3. After that, the slides were immersed in hematoxylin for 3 minutes at room temperature and washed in running tap water for 3 minutes.

4. The slides were immersed in eosin for 5 seconds at room temperature and dehydrated by moving the slide through 2 chambers of 95% alcohol and 2 chambers of xylene, respectively for 10 seconds in each chamber. After dehydration, the slides were mounted with a mounting medium.

All samples were evaluated by an experienced pathologist who is blinded to the experiment. All fields in each section were examined for grading of steatosis and necroinflammation according to Colantoni et al.'s criteria (Colantoni et al., 2003)

Steatosis was scored as the percentage of parenchymal cells containing fat (micro-or macrosteatosis).

0 = no parenchymal cells containing fat

1 = <20% of parenchymal cells containing fat

2 = 20–39% of parenchymal cells containing fat

3 = 40–50% of parenchymal cells containing fat

4 = >51% of parenchymal cells containing fat

Inflammation and necrosis were scored by the number of foci of inflammation and necrosis identified under low-power field of light microscope.

0 = no inflammation and necrosis

1 = 1 focus per low-power field of inflammation and necrosis

2 = 2 foci per low-power field of inflammation and necrosis

3 = 3 or more foci per low-power field of inflammation and necrosis

2. Hepatic Malondialdehyde (MDA) Determination

MDA was measured from the homogenized tissue by using thiobarbituric acid (TBA) reaction as described by Ohgawa et al. (Ohgawa et al., 1979). The basic principle of the method is the reaction of one molecule of MDA and two molecules of TBA to form a red MDA-TBA complex, which can be quantitated spectrophotometrically (532 nm).

Procedure

1. One gram of liver was placed in a test tube containing 9.0 ml of 1.15% KCl buffer and homogenized on an ice box using a homogenizer at a rotational speed of 12,000 rpm for 1 minute. The homogenate was collected and aliquot into sterile microcentrifuge tubes for detecting MDA and protein assay.

2. For standard curve preparation, malondialdehyde bis solution was used as an external standard. The level of lipid peroxide was expressed as nmol of MDA. A stock solution of 10^{-3} M MDA was prepared with distilled water and a series of standards (duplication) was set as described below.

Tube	Stock MDA (ml)	DW (ml)	Final MDA concentration (M)	MDA in 0.2 ml solution (nmol)
1	0.10	9.90	1.0×10^{-5} M	2
2	0.25	9.75	2.5×10^{-5} M	5
3	0.50	9.50	5.0×10^{-5} M	10
4	0.75	9.25	7.5×10^{-5} M	15
5	1.00	9.00	10.0×10^{-5} M	20

3. The following solutions and samples were pipetted into tubes with screw caps.

Solution	Blank:DW (ml)	Standard (ml)	Unknown (ml)
Sample	-	-	0.2
8.1% SDS	0.2	0.2	0.2
20% Acetic acid (pH 3.5)	1.5	1.5	1.5
0.8% TBA	1.5	1.5	1.5
MDA stock standard	-	0.2	-
Distilled water	0.8	0.6	0.6

Note: DW = Distilled water

4. The tubes were heated in the water-bath at 95°C for 60 minutes.

5. After cooling the tubes by immersion with tap water, 1.0 ml of distilled water and 5.0 ml of the mixture of n-butanol and pyridine (15:1, v/v) were added and shaken vigorously (at least 1 minute).

6. After centrifugation at 4,000 rpm for 10 minutes, the absorbance of the organic layer (upper layer) was measured at 532 nm.

Calculation

A standard curve was created by plotting the mean absorbance for each standard on the y-axis against the nmol of MDA on the x-axis (Figure 3-16). MDA levels of the samples were determined from the linear regression equation of a standard curve. The content of lipid peroxide is expressed in term of nmol of MDA/gram of wet weight and the total protein was determined by the Lowry method (Lowry et al., 1951) to correct the MDA level which is expressed in terms of nmol/mg protein.

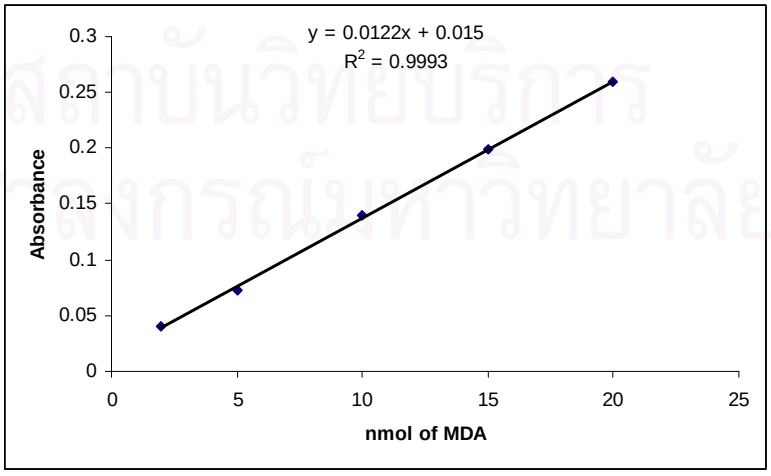

Figure 3-16. Example of standard curve

3. Hepatic Superoxide Dismutase (SOD) Activity

SOD was determined using the method of Winterbourn (Winterbourn et al., 1975), in which the light-triggered release of superoxide radicals from riboflavin leads to the formation of a blue complex through reaction with nitroblue tetrazolium (NBT).

Procedure

1. One gram of liver was placed in a test tube containing 9.0 ml of 0.1 M phosphate buffer saline (PBS) pH 7.4 and homogenized using a homogenizer at a rotational speed of 12,000 rpm for 1 minute under ice cool condition.

2. The homogenate was centrifuged at 3,000 rpm for 15 minutes at 4^{0}C and the supernatant was collected and aliquot into sterile microcentrifuge tubes for detecting SOD activity and protein assay. For detecting SOD activity, samples were diluted with PBS (1:16)

3. The reagents and sample were added into 8 test tubes as follows:

No. of Tube	Sample (μl)	0.067 Phosphate buffer, pH7.8 (ml)	0.1 M EDTA (ml)	1.5 mM NBT (ml)	0.12 mM Riboflavin (ml)
1	0	2.65	0.2	0.1	0.05
2	10	2.64	0.2	0.1	0.05
3	20	2.63	0.2	0.1	0.05
4	40	2.61	0.2	0.1	0.05
5	60	2.59	0.2	0.1	0.05
6	80	2.57	0.2	0.1	0.05
7	200	2.45	0.2	0.1	0.05
8	500	2.15	0.2	0.1	0.05

Note- NBT and riboflavin were added in a dark room

- riboflavin was added last.

4. The tubes were mixed and placed in an illuminated chamber with an 18 W fluorescent lamp for 12 minutes at room temperature. Optical density was measured at 560 nm.

Calculation

1. Percentage inhibition of each volume of sample was calculated from this formula below and created the percentage inhibition of NBT reduction curve by plotting percentage inhibition of NBT reduction for each volume of sample on the y-axis against the each volume of sample on the x-axis (Figure 3-17).

$$\% \text{ inhibition} = \frac{\text{O.D. of control (tube No.1) - O.D. of sample}}{\text{O.D. of control (tube No.1)}} \times 100$$

2. The volume of sample which gave half of the maximum percentage inhibition was 1 unit. The SOD activity was calculated from the formula below and the results were expressed as units/mg protein.

$$\text{Units} = \frac{100{,}000 \times \text{dilution factor}}{\text{Volume} \times \text{mg protein}}$$

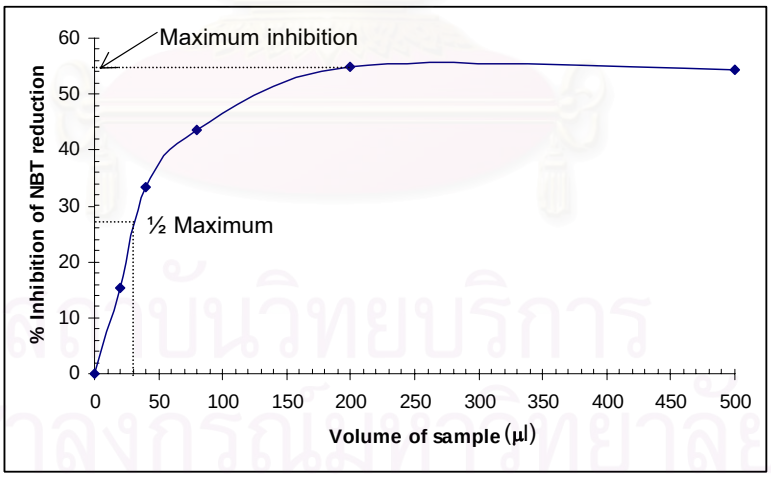

Figure 3-17. Example of inhibition of NBT reduction

4. Hepatic Apoptosis Determination

The DNA fragmentation is characteristic apoptotic cell which is detected by TdT-mediated X-dUTP nick end labeling (TUNEL) assay (ApopTag® Plus Peroxidase *In Situ* Apoptosis Detection Kit, Chemicon, USA). In principle, the terminal deoxynucleotidyl transferase (TdT) catalyzes a template-independent addition of nucleotide triphosphates to the 3'-OH ends of double-stranded or single-stranded DNA. The incorporated nucleotides form an oligomer composed of digoxigenin-conjugated nucleotide and unlabeled nucleotide in a random sequence. DNA fragments which have been labeled with the digoxigenin-nucleotide are then allowed to bind an anti-digoxigenin antibody that is conjugated to a peroxidase reporter molecule. The bound peroxidase antibody conjugate enzymatically generates a permanent, intense, localized stain from chromogenic substrates, providing sensitive detection in immunohistochemistry.

Procedure

1. Tissue Preparation

Liver sections of 5 μm thick from paraffin-embedded blocks were put on slides and deparaffinized in 3 changes of xylene for 5 minutes. The slides were hydrated in 3 changes of 95% alcohol for 5 minutes and washed in one change of PBS pH 7.4 in a coplin jar for 5 minutes. The slides should not be allowed to dry out at any point during procedure.

2. Pretreatment of Tissue

Freshly diluted proteinase K (1:10) was applied on the slides (200 μl/slide) for 10 minutes at room temperature in order to suffice permeabilization of cells, so TUNEL reagents can reach nuclei. Then, the slides were washed in 2 changes of distilled water in a coplin jar for 2 minutes per wash. 3% H_2O_2 was applied on the slides (200 μl/slide) for 5 minutes at room temperature to block endogenous peroxide activity. The slides were rinsed in 2 changes of distilled water in a coplin jar for 5 minutes each wash.

3. Application of TUNEL Reagents

The slides were gently tapped off excess distilled water and equilibration buffer (50 μl/slide) immediately applied directly on slides for at least 10 seconds at room temperature. Next, working strength TdT enzyme was applied on the slides (50 μl/slide)

and the slides were incubated in a humidified chamber at 37°C for 1 hour. After incubation, the slides were put in a coplin jar containing working strength stop/wash buffer, agitated for 15 seconds and incubated for 10 minutes at room temperature. The slides were washed in 3 changes of PBS for 1 minute each wash and gently tapped off excess liquid. Anti-digoxigenin-peroxidase was applied on the slides (50 μl/slide) for 30 minutes in humidified chamber at room temperature. Then, the slides were washed in 4 changes of PBS for 2 minutes per wash and gently tapped off excess liquid.

4. Color Development and Counterstain

3,3' diaminobenzidne (DAB) was applied on the slides (50 μl/slide) for 5 minutes at room temperature and the slides were washed in 3 changes of distilled water for 1 minute per wash. After that, the slides were immersed in hematoxylin for 10 seconds at room temperature and run with tap water for 1 minute. Then, the slides were immersed in 0.1% lithium carbonate for 3 seconds and dehydrated by moving the slide through 2 chambers of 95% alcohol and 2 chambers of xylene, respectively for 10 seconds in each chamber. After dehydration, the slides were mounted with a mounting medium.

Under light microscopy, the positive stained cells presented dark brown nuclei. All fields of each sample were evaluated for hepatic apoptosis and the results were expressed as the number of apoptosis cells per high-power field.

5. Immunohistochemmistry for Expression of NF-κB p65 in Liver

Immunohistochemistry is a method used for localizing proteins in or on cells of a tissue section using the principle of antibodies binding specifically to antigens. It has a two-step process involving first, the binding of the antibody to the antigen of interest, and second, the detection and visualization of bound antibody by one of a variety of enzyme chromogenic systems. Classically, a secondary antibody is conjugated to an enzyme, such as peroxidase, that can catalyse a color-producing reaction.

Procedure

1. Tissue Preparation

Liver sections of 5 μm thick from paraffin-embedded blocks were put on slides and deparaffinized in 3 changes of xylene for 5 minutes. The slides were hydrated

in 3 changes of 95% alcohol for 5 minutes and run with tap water for 3 minutes. The slides should not be allowed to dry out at any point during procedure.

2. Pretreatment of Tissue

Certain antigenic determinants are masked by formalin fixation and paraffin embedding. Recovery of antigens in paraffin sections often can be accomplished by heat treatment. The slides were put in a coplin jar containing 10 mM citrate buffer pH 6.0 and heated in microwave for 13 minutes. Then, the slides were allowed to cool in the buffer for 20 minutes and washed in 3 changes of PBS pH 7.4 for 2 minutes each wash in a chamber. 3% H_2O_2 was applied on the slides (200 μl/slide) for 5 minutes at room temperature to block endogenous peroxide activity. After that, the slides were run with tap water for 5 minutes and nonspecific background was minimized by incubating with 3% normal horse serum in PBS for 20 minutes at room temperature. Next, the slides were immersed in PBS for 3 minutes in a chamber.

3. Application of Primary Antibody and Second Antibody

The slides were gently tapped off excess liquid and primary antibody (NF-κB p65, Santa Cruz Biotechnology, USA) was applied at a dilution 1:150 on the slides (200 μl/slide) for 1 hour at room temperature. After incubation, the slides were washed in 3 changes of PBS for 3 minutes each wash in a chamber and gently tapped off excess liquid. Super Enhancer® Reagent (Super Sensitive Polymer-HRP Detection Kit, BioGenex, CA) was added to cover the specimens (200 μl/slide) for 20 minutes at room temperature and slides were rinsed in 3 changes of PBS for 3 minutes each in a chamber. Then, Poly-HRP Reagent (Super Sensitive Polymer-HRP Detection Kit, BioGenex, CA) was applied on the slides (200 μl/slide) for 30 minutes at room temperature and slides were washed in 3 changes of PBS for 3 minutes per wash in a chamber and gently tapped off excess liquid.

4. Color Development and Counterstain

DAB was applied on the slides (200 μl/slide) for 10 minutes at room temperature and the slides were run with tap water for 5 minutes. After that, the slides were immersed in hematoxylin for 10 seconds at room temperature and run with tap water for 1 minute. Then, the slides were immersed in 0.1% lithium carbonate for 3 seconds and dehydrated by moving the slide through 2 chambers of 95% alcohol and 2

chambers of xylene, respectively for 10 seconds in each chamber. After dehydration, the slides were mounted with a mounting medium.

Under light microscopy, the positive stained cells presented dark brown nuclei. All fields of each sample were evaluated and the results were expressed as the number of positive stained cells per high-power field.

6. Western Blot Analysis of PPARγ and α-SMA Protein Expression in Liver

The term "blotting" refers to the transfer of biological samples from a gel to a membrane and their subsequent detection on the surface of the membrane. Western blotting (also called immunoblotting because an antibody is used to specifically detect its antigen) was introduced by Towbin, et al. in 1979 and is now a routine technique for protein analysis. The specificity of the antibody-antigen interaction enables a target protein to be identified in the midst of a complex protein mixture. Western blotting can produce qualitative and semiquantitative data about that protein. The first step in a Western blotting procedure is to separate the macromolecules using polyacrylamide gel electrophoresis (PAGE). After electrophoresis, the separated molecules are transferred onto a second matrix, generally a nitrocellulose or polyvinylidene difluoride (PVDF) membrane. Next, the membrane is blocked to prevent any nonspecific binding of antibodies to the surface of the membrane. The transferred protein is complex with an enzyme-labeled antibody as a probe. An appropriate substrate is then added to the enzyme and together they produce a detectable product such as a chromogenic precipitate on the membrane for colorimetric detection. The most sensitive detection methods use a chemiluminescent substrate that, when combined with the enzyme, produces light as a byproduct. The light output can be captured using film or a CCD camera that is designed for chemiluminescent detection.

Procedure

1. Protein Extraction

Frozen livers (0.1 gram) were homogenized with lysis buffer (see Appendix B) on an ice box using a homogenizer at a rotational speed of 12,000 rpm for 1 minute. The homogenates were centrifuged at 12,000 rpm for 15 minutes at 4^0C and

supernatant was collected and aliquot into sterile microcentrifuge tubes for detecting PPARγ, α-SMA protein expression and protein assay.

2. Sodium Dodecyl Sulfate-Polyacrylamide Gel Electrophoresis (SDS-PAGE)

In SDS-PAGE applications, the sample applied to the slab gel has been treated with the detergent SDS. This ionic detergent denatures the proteins in the sample and binds tightly to the uncoiled molecule. The SDS molecules mask the intrinsic charge of the protein and create a relatively uniform negative charge distribution caused by the sulfate groups on SDS. When an electric current is applied, all proteins will migrate through the gel toward the anode, which is placed at the bottom of the gel. The SDS-PAGE gel separates proteins primarily according to size because the SDS-coated proteins have a uniform charge: mass ratio. Proteins with less mass travel more quickly through the gel than those with greater mass because of the sieving effect of the gel matrix. Protein molecular weights can be estimated by running standard proteins of known molecular weights in a separate lane of the same gel.

3. Preparation of Slab Gel

The sandwich plates (SE 260 mini-vertical gel electrophoresis unit, Amersham, USA) were set up for casting the gel. For separating gel, 10% acrylamide solution (see Appendix B) was carefully filled into the gap between the sandwich plates. The height of separating gel was adjusted by the comb, approximately 1 cm below the length of the teeth of the comb. The top layer was filled with 1 ml of distilled water. The gel was placed to polymerize at room temperature for 30 minutes. After polymerization, the water was drained off and the comb was inserted gently. Then 5% acrylamide solution (see Appendix B) was filled into the gap for making the stacking gel and the gel was placed to polymerize at room temperature for 20 minutes.

4. Preparation of Sample and Running the Gel

While the stacking gel was polymerizing, equal amounts of total protein from each sample were mixed with sample buffer (2X) (see Appendix B) and heated for 5 minutes at 95^{o}C in heat box. After polymerization was completed (20 minutes), the comb was removed carefully and the gel was mounted in the electrophoresis apparatus (Figure 3-18a). The running buffer (see Appendix B) was filled into the upper and lower

chamber. The amount of 60 μg of each protein sample was loaded into the bottom of the wells and 5 μl of the molecular weight marker was also loaded. The electrophoresis apparatus was attached to an electric power supply and applied 0.02 amperes to the gel (Figure 3-18b). After the dye front reached the bottom of separating gel (~1 hour), the power supply was turned off. The gel was removed from sandwich plates and the area of stacking gel was cut away by gel spacer.

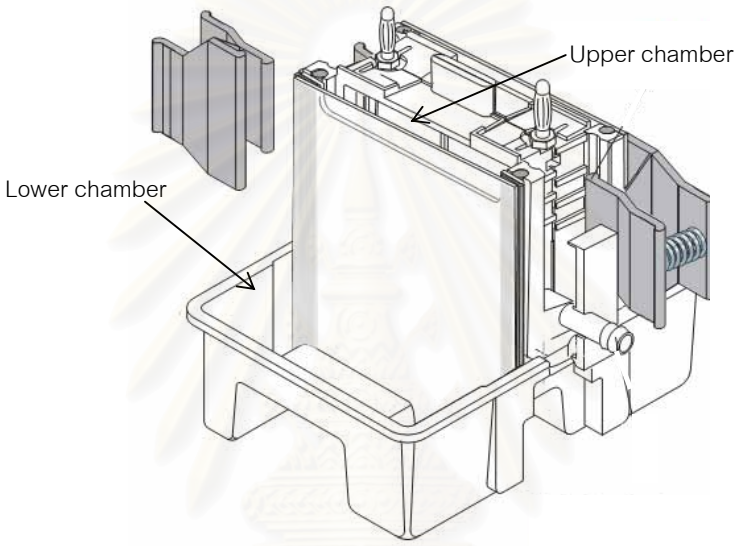

a

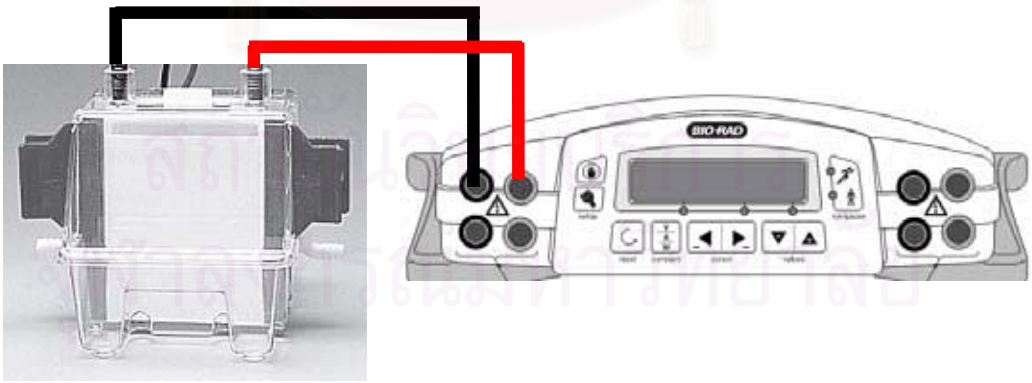

b

Figure 3-18. The electrophoresis apparatus with gel sandwich installation (a) and attached to the power supply (b) (http://www.hoeferinc.com/downloads/SE260-IM.pdf)

5. Transfer of Protein to a Membrane

A PVDF membrane and six thick blotting papers were cut into the same size of gel and soaked in transfer buffer (see Appendix B) for 10 minutes. To assemble the transfer sandwich, three thick blotting papers, membrane, gel and three thick blotting papers were placed, respectively on the platinum anode of the Tran-Blot SD semi-dry electrophoretic transfer cell (Bio-Rad, USA). Then, a clean pipette was used to roll out the air bubbles and the amount 3 ml of transfer buffer was added on top of sandwich. The stainless-stell cathode assembly was latched on top of sandwich. Then, the safety cover was placed onto the unit and plugged into the electric power supply which applied 15 voltages for 45 minutes (Figure 3-19).

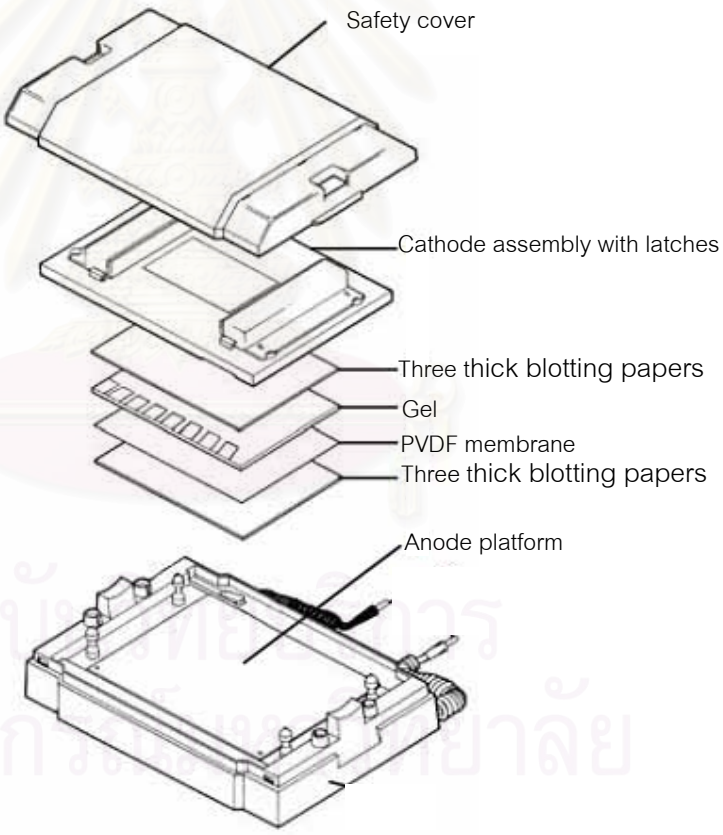

Figure 3-19. Transfer cell assembly

(http://www.genmall.com.tw/products/INFO/Bulletin_2134B%20Increased%20Transfer%20Efficiency%20Using%20a%20Discontinuous%20Buffer%20System%20With%20the%20Trans-Blot%20SD%20Cell%20Rev%20B.pdf)

6. Block Nonspecific Binding Sites

The membrane was removed from transfer sandwich and incubated in blocking solution (5% skim milk in TBS) for 1 hour at room temperature on a platform rocker. This process reduces the background of nonspecific binding site with irrelevant protein. After blocking, the membrane was washed 2 times for 5 minutes each with TBS-0.1% Tween 20 (wash buffer) (see Appendix B) on a platform rocker.

7. Primary and Secondary Antibody Incubation

The dilution of primary and secondary antibody were prepared in 1% skim milk in TBS (1:400 for PPARγ, 1:5,000 for β-actin, 1:1,000 for α-SMA and 1:4,000 for secondary antibody). The membrane was incubated with diluted primary antibody overnight at 4°C on a platform rocker, and then the diluted primary antibody was discarded. The membrane was washed with wash buffer for 5 minutes 3 times and incubated with diluted secondary antibody (Goat anti-mouse IgG HRP) for 1 hour at room temperature on a platform rocker. After incubation, the membrane was washed with wash buffer for 5 minutes 3 times.

8. Protein Detection

The detection reagent (ECL plus western blotting detection reagent, Amersham, USA) was prepared by mixing solution A and B in a ratio of 40:1 in a dark place. The excess wash buffer was drained from the washed membrane and the membrane was placed on glass plate. The mixed detection reagent was pipetted on to the membrane and incubated for 5 minutes at room temperature. The excess detection reagent was drained off by holding the membrane gently in forceps and touching the edge against a tissue. The membrane was wrapped by a fresh piece of plastic. It is necessary to work quickly once the membrane has been exposed to the detection reagent. In a dark room, the membrane was placed, protein side up, in an X-ray film cassette and a sheet autoradiography film was placed carefully on the top of the membrane. The cassette was closed and exposed for a certain period (30 minutes for PPARγ and α-SMA, 5 minutes for β-actin). The film was developed by manual processing. The film was attached to forceps and moved from developer solution, water, fixer solution and water, respectively by hand. The intensity of band was scanned by

using high resolution scanner and each intensity band was quantified by Scion Image program. The intensity ratio of each studied protein to β-actin was calculated.

9. Image Analysis

9.1 Scion Image program was opened and special menu was selected. Then, load macro file was opened that showed macro folder of Scion Image. Gelplot2 was picked in macro folder and picture file was opened to mark the interesting lanes as showed below (Figure 3-20).

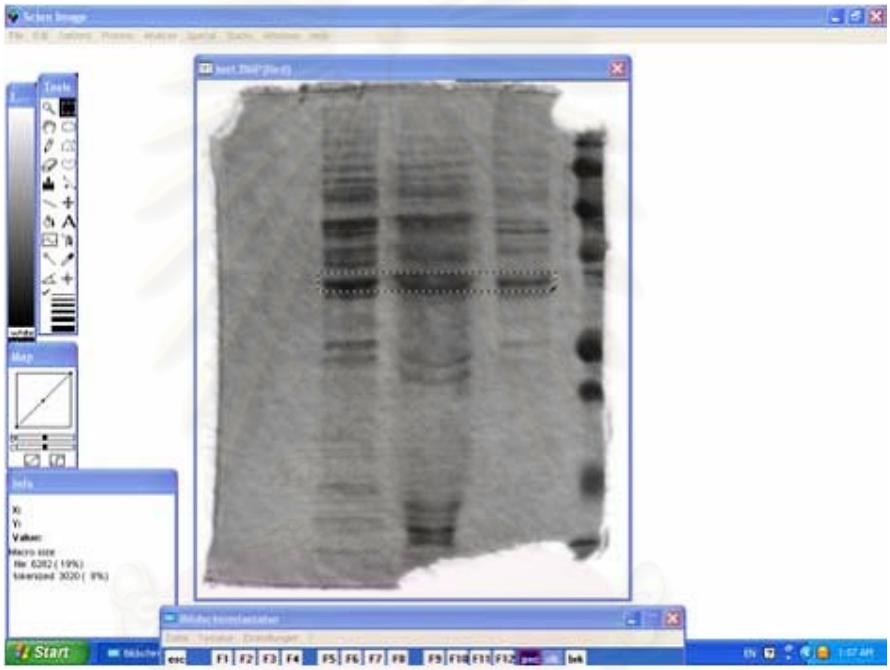

Figure 3-20. The selected lanes

9.2 Special menu was selected and mark first lane [1] was picked. A new window appeared with a zoom in of the desired area. In special menu, plot lane [3] was opened and the program counted the number of black pixels against the background and a graphical result appeared (Figure 3-21).

9.3 To quantify the concentration differences between each lane, the lanes from one another were separated by drawing lines with the line tool as showed below (Figure 3-22).

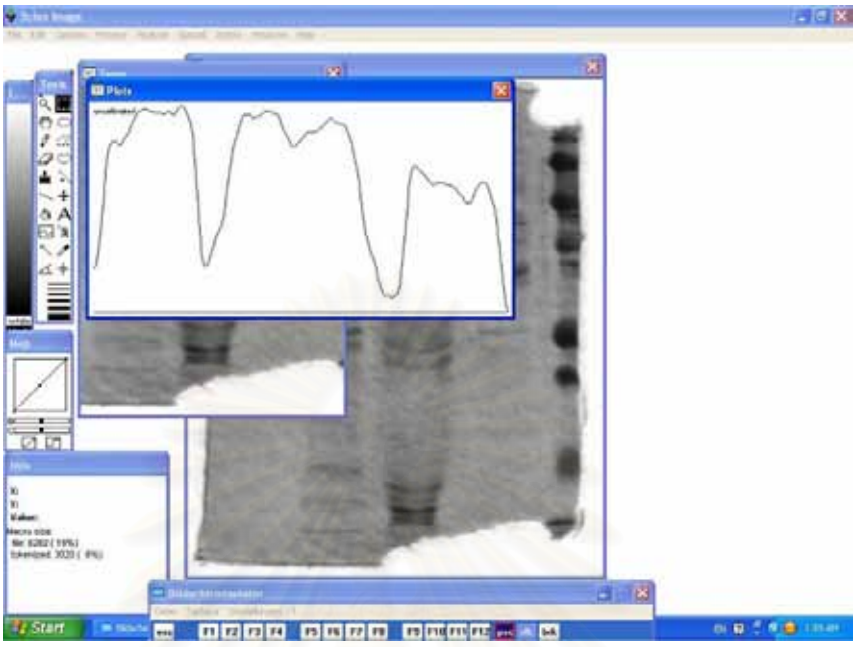

Figure 3-21. The showed plot results

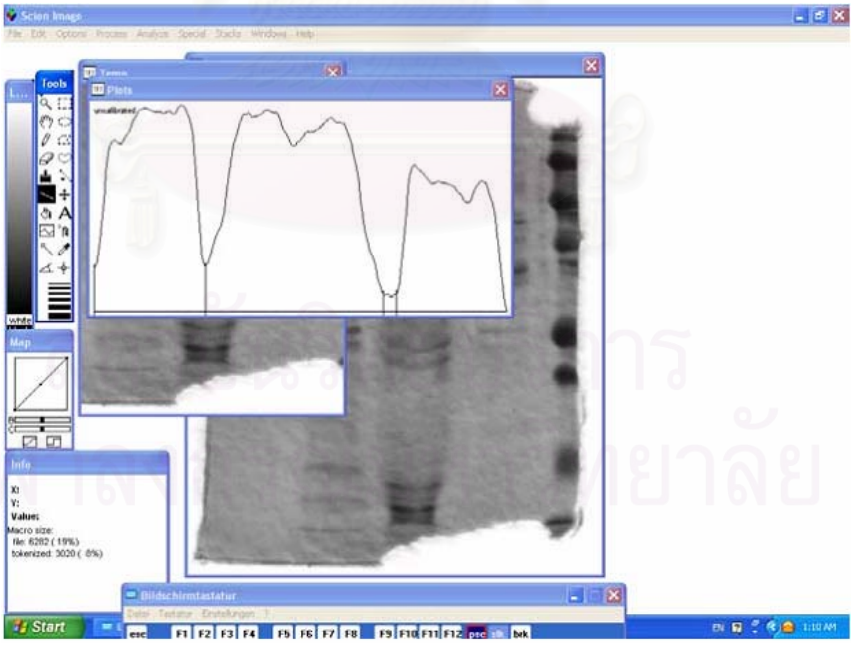

Figure 3-22. Lane specification

9.4 The each lane was a different entity. With the magic wand (second tool from bottom to top on the left side of the tools menu) selected consecutively each of the separate areas once.

9.5 In analyze menu, show result was selected. Scion Image would measure the area of each selected part of the graph and gave as numerical results.

7. Protein Assay (Lowry Method)

The principle lines are in the reactivity of the peptide bond of protein with the copper II ion (divalention) under alkaline conditions and reduced to copper I ion (monovalention). Copper I ion and the radical groups of tyrosine, tryptophan and cysteine amio acid side chains of protein (the protein-copper complex) react with the folin phenol reagent (phosphomolybdic-phosphotungstic acid) to produce heteropolymolybdenum blue by the copper catalyzed oxidation of aromatic acid and change blue color which is analyzed by visible spectrophotometer (Lowry et al., 1980).

Reagents

1. Solution A (alkaline tartrate reagent)

Na_2CO_3	10.0	g
$Na_2C_4H_4O_6.2H_2O$	0.1	g
NaOH	1.2	g

These chemicals were dissolved in distilled water and made up 500 ml.

2. Solution B (0.5% copper sulfate): 0.5 g of $CuSO_45H_2O$ was dissolved in 100 ml distilled water.

3. Solution C (prepare fresh, within 1 day of use): 500 ml of solution A was added in 10 ml of solution B and mixed well.

4. Solution D (1 N folin phenol reagent): 30 ml of 2 N folin ciocalteu's phenol reagent was added in 30 ml of distilled water.

5. Standard protein solution (bovine serum albumin,BSA, 1 mg/ml)

Procedure

1. A series of standards (duplication) which contain 0, 50, 100, 250 and 500 μg/ml of BSA were set as described below

The BSA was prepared as stock at concentration of 1 mg/ml. Standard curve was prepared as showed below.

Tube	BSA stock (μl)	DW (ml)	Final BSA Concentration(μg/ml)
1	0	1.2	0
2	62.5	1.1875	50
3	125	1.125	100
4	312.5	0.9375	250
5	625	0.625	500

2. Samples were diluted with buffer (1:100) and mixed well. Then solutions and samples were added into tubes with screw caps as follows:

Solution	Blank:DW (ml)	Standard (ml)	Unknown (ml)
Distilled water	0.5	-	-
BSA	-	0.5	-
Diluted sample	-	-	0.5
Solution C	5.0	5.0	5.0

3. All tubes were mixed well and stood at room temperature for 10 minutes. Later, the amount of 0.5 ml of solution D was added and the tubes were stood for 30 minutes at room temperature.

4. The absorbance of each solution was read and recorded at 750 nm. Protein concentration which was multiplied by a dilution factor is expressed as μg/ml.

Data Analysis

Data were presented as means ± standard deviation (SD) for continuous data and frequency for categorical data (score of steatosis and necroinflammation). One way analysis of variance (one-way ANOVA) and Tukey post hoc comparisons were used to compare normally distributed data among all groups. Kruakal-Wallis Test and

Mann-Whitney test was employed to compare abnormal distributed data. Differences were considered statistically significant at $p<0.05$.

CHAPTER IV

RESULTS

1. Body Weight of Rats

Alcohol group lost weight significantly compared with Control group after the end of the experiment (212.0±33.4 vs. 246.6±7.9 g, $p<0.05$). The weight loss was apparent immediately after starting the alcohol feeding and correlated with reduction of food intake at the first week (Figure 4-23 and 4-24). However, rats increased food intake after the second week and the body weight of rats was stabilized after the third week. For Alcohol+curI and Alcohol+curII, there was no significant difference in body weight at the end of experiment compared with control group (248.8±14.4 vs. 246.6±7.9 g, 254.4±13.6 vs. 246.6±7.9 g respectively; $p<0.05$). Despite weight loss, the general condition of Alcohol group remained good throughout the experiments.

2. Histopathological Examination

The histologic appearance of the liver in Control group was normal (Figure 4-25a). Alcohol group demonstrated a significant fat accumulation and mild inflammatory cells infiltration (Figure 4-25b) while Alcohol+curI and Alcohol+curII improved the liver histopathology (Figure 4-25c and 4-25d). Histologic score of steatosis and necroinflammation were summarized in Table 4-3.

3. Hepatic MDA Level

The level of hepatic MDA increased significantly in Alcohol group as compared with Control rats (3.42±1.36 vs. 1.44±0.24 nmol/mg protein, $p<0.05$). Alcohol+curI and Alcohol+curII decreased the elevation of hepatic MDA level significantly when compared with Alcohol group (1.43±0.14, 1.43±0.29 vs. 3.42±1.36 nmol/mg protein, respectively; $p<0.05$) (Figure 4-26).

4. Hepatic SOD Activity

The level of hepatic SOD activity of the Control group was 1081.36±145.01 units/mg protein, while that of the Alcohol group was 1135.86±209.48 units/mg protein. For Alcohol+curI and Alcohol+curII groups the levels of hepatic SOD activity were 966.28±139.44 and 967.84±116.66 units/mg protein, respectively. There was no significant difference among groups (Figure 4-27).

5. Hepatic Apoptosis

The number of apoptotic nuclei in the liver of Control was very low (0.38±0.28 cells/high-power field). In contrast, the number of apoptotic cells were observed frequently in centrilobular area in Alcohol group when compared with Control (2.43±2.68 vs. 0.38±0.28 cells/high-power field, $p<0.05$). The number of apoptotic cells in the liver of Alcohol+curI group was lower than Alcohol group, but the difference did not reach a statistical significance. The number of apoptotic cells was significantly increased in Alcohol+curII group when compared with Control group (2.08±2.35 vs. 0.38±0.28 cells/high-power field) (Figure 4-28 and Figure 4-29).

6. Expression of NF-κB p65 in Liver

The data of NF-κB p65 expression in all groups were given in Figure 4-30. The number of positive stained cells in the liver of Alcohol group were significantly higher than Control (1.08±0.52 vs. 0.04±0.04 cells/ high-power field, $p<0.05$). In contrast, Alcohol+curI and Alcohol+curII groups inhibited the number of positive stained cells significantly when compared with Alcohol group (0.15±0.02 vs. 1.08±0.52 and 0.17±0.09 vs. 1.08±0.52 cells/ high-power field, respectively; $p<0.05$) (Figure 4-30 and 4-31).

7. PPARγ Protein Expression in Liver

In order to examine the change of PPARγ protein expression in early stage of alcohol-induced liver injury, we measured PPARγ protein expression in the liver. The PPARγ protein expression in Control group was 0.57±0.19 and Alcohol group was 0.68±0.16. Alcohol+curI and Alcohol+curII groups had 0.44±0.03 and 0.54±0.23,

respectively. These data did not show a significant change in PPARγ protein expression in the liver in all groups (Figure 4-32).

8. α-SMA Protein Expression in Liver

In order to examine HSC activation that represents liver fibrosis. We measured α-SMA protein expression in the liver. The α-SMA protein expression in Control group was 0.61±0.30 and Alcohol group was 0.63±0.15. The Alcohol+curI and Alcohol+curII groups had 0.72±0.27 and 0.60±0.25, respectively. These data did not show a significant change in α-SMA protein expression in the liver in all groups (Figure 4-33). Thus, this model showed no HSC activation.

Table 4-3. Summary of steatosis and necroinflammation score in all groups (number)

Group	Steatosis					Necroinflammation			
	0	1	2	3	4	0	1	2	3
Control (n=8)	8	-	-	-	-	8	-	-	-
Alcohol (n=8)	-	1	6	1	-	-	8	-	-
Alcohol+curl (n=6)	5	1	-	-	-	6	-	-	-
Alcohol+curII (n=7)	4	3	-	-	-	3	4	-	-

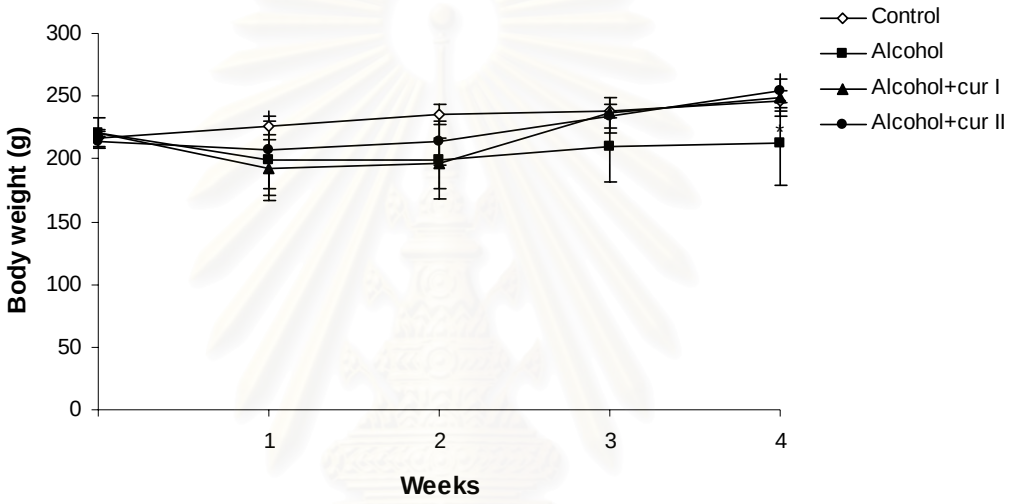

Figure 4-23. Body weight of animal in all groups (mean±SD)

*significant difference ($p<0.05$) compared with Control

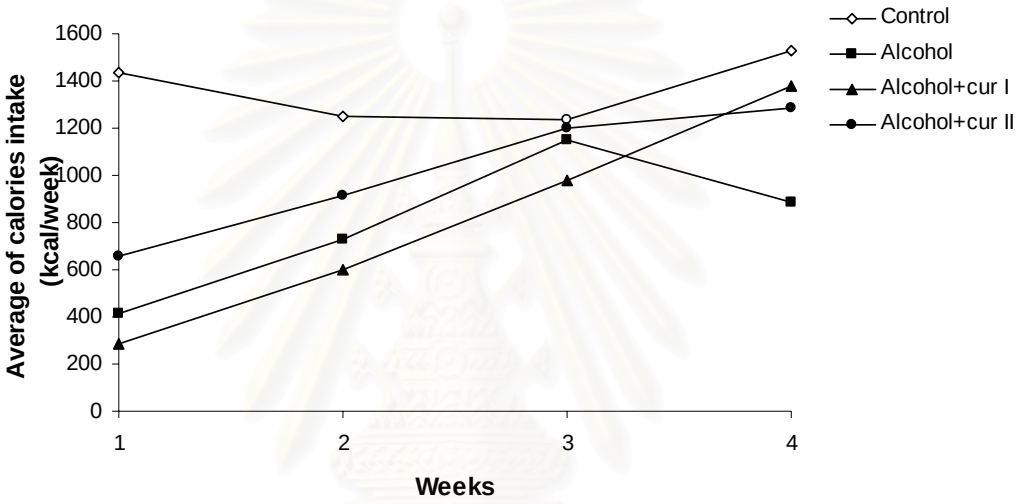

Figure 4-24. Calories consumed by each group (mean)

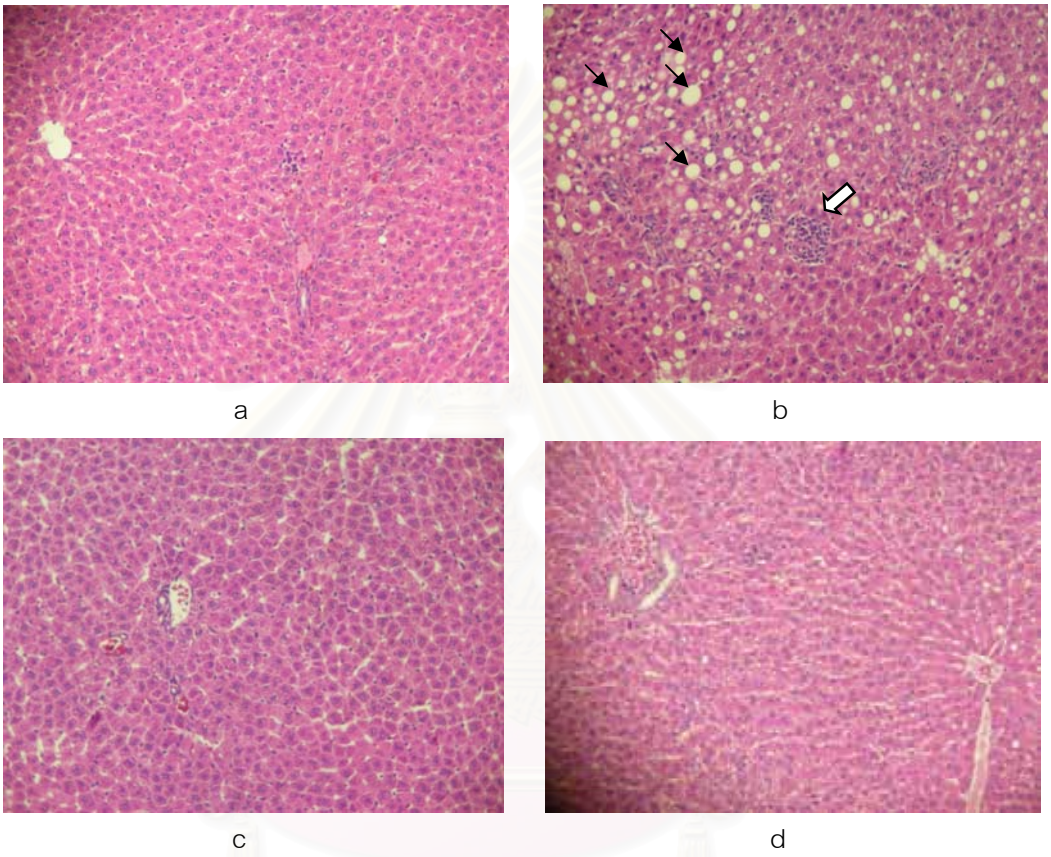

Figure 4-25. Hematoxylin-eosin stained liver sections (x400). a) Control group showed normal liver histopathology. b) Alcohol group showed steatosis (small arrows) and infiltration of inflammatory cells (block arrow). c) and d) Alcohol+curI and Alcohol+curII groups showed examples of improvement in steatosis and inflammation.

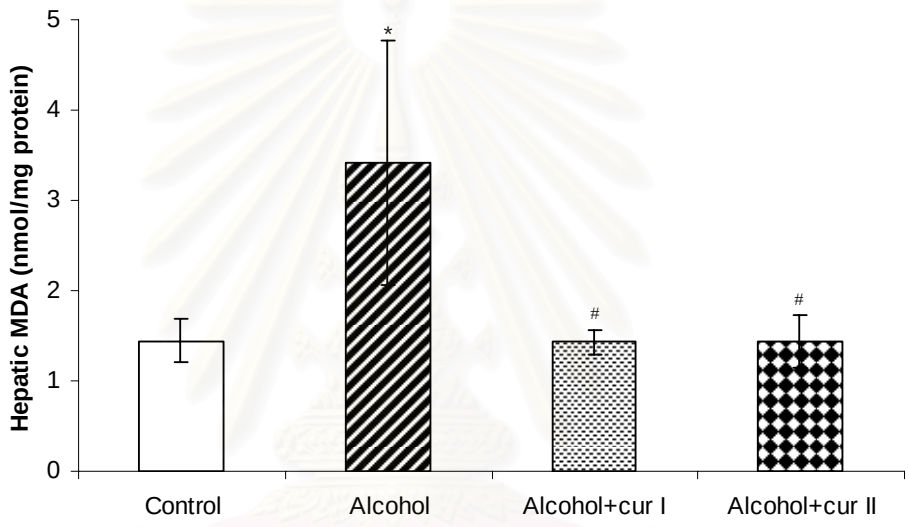

Figure 4-26. Hepatic MDA levels in all groups (mean±SD)

* significant difference ($p<0.05$) compared with Control

significant difference ($p<0.05$) compared with Alcohol

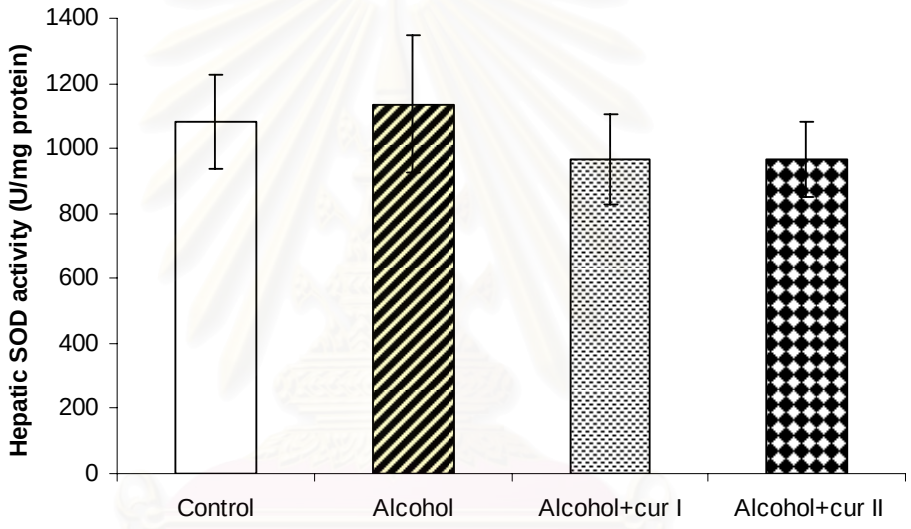

Figure 4-27. Hepatic SOD activity in all groups (mean±SD)

Figure 4-28. Number of apoptosis cells in all groups (mean±SD)

* significant difference ($p<0.05$) compared with Control

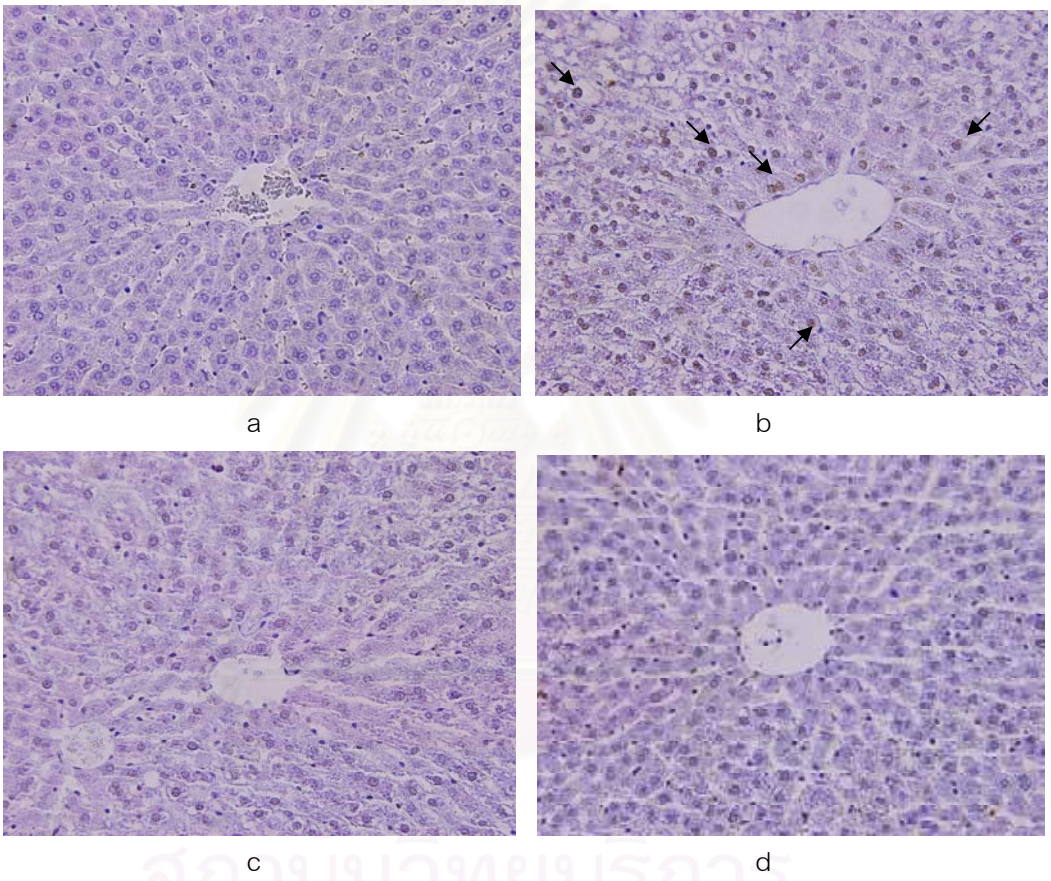

Figure 4-29. Representative liver sections processed for apoptosis assay by TUNEL reaction (x400). a) Control group. b) Alcohol group, the black arrows indicated a TUNEL-positive apoptoic hepatocyte frequently found around central vein. c) and d) Alcohol+curl and Alcohol+curlI groups showed a decrease of apoptotic hepatocytes.

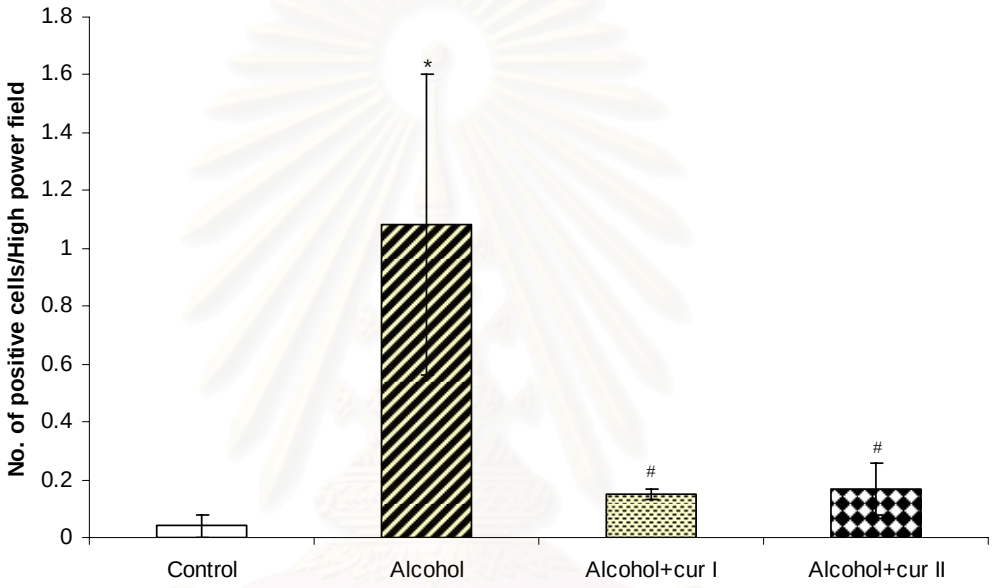

Figure 4-30. Number of NF-κB p65 positive cells/high-power field in all groups (mean±SD)

* significant difference ($p<0.05$) compared with Control

significant difference ($p<0.05$) compared with Alcohol

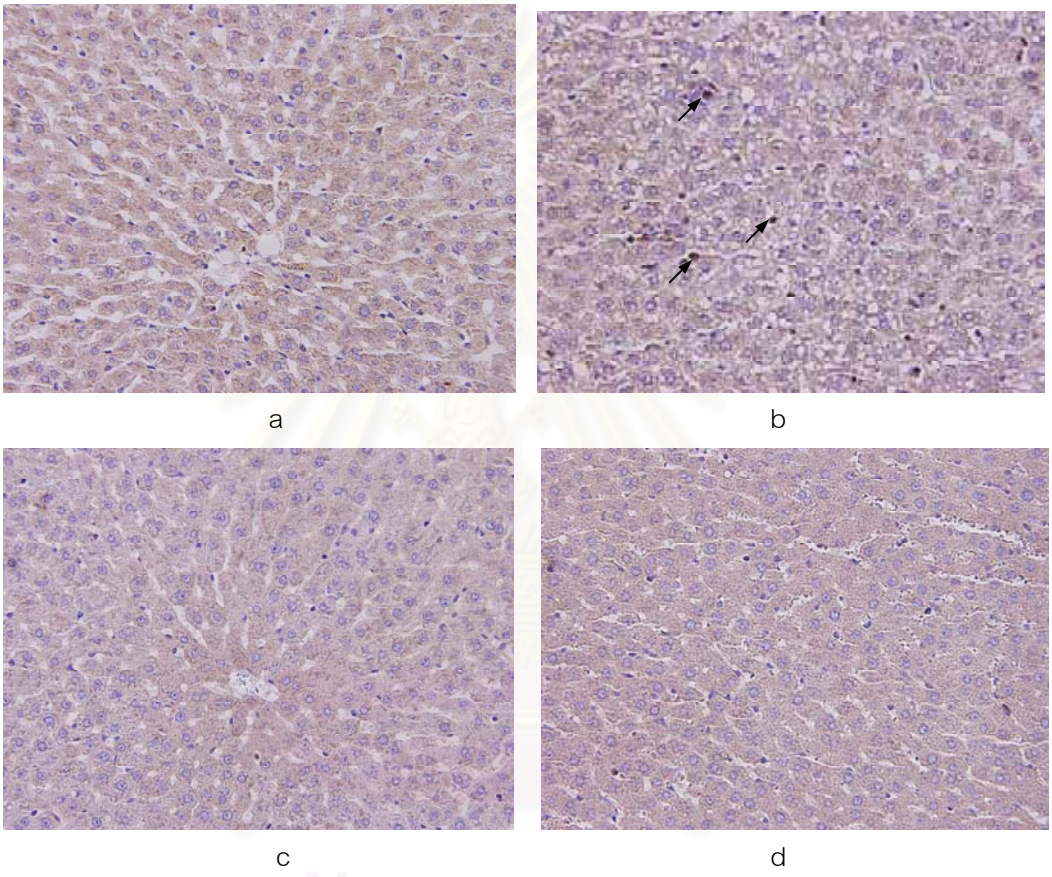

Figure 4-31. Immunohistochemistry of NF-κB p65 expression in rat liver (x400). a) Control group. b) Alcohol group showed NF-κB p65 positive cells in nuclei (black arrow). c) and d) Alcohol+curI, Alcohol+curII groups showed a diminishment of NF-κB expression in hepatocyte nuclei.

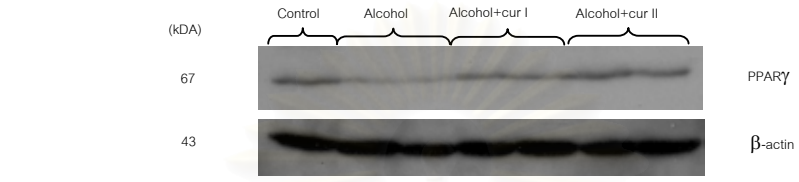

a

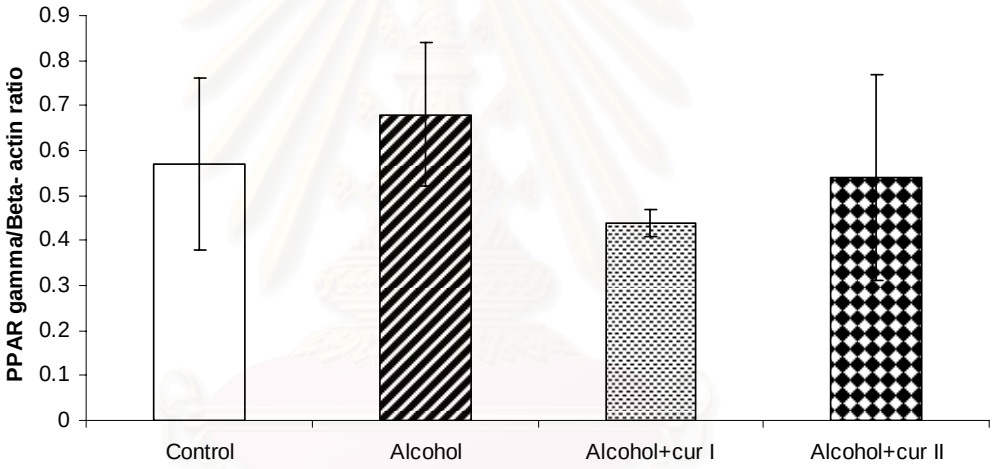

b

Figure 4-32. Representative blot of PPARγ expression (a) and the ratio to β-actin in all groups (b) (mean±SD)

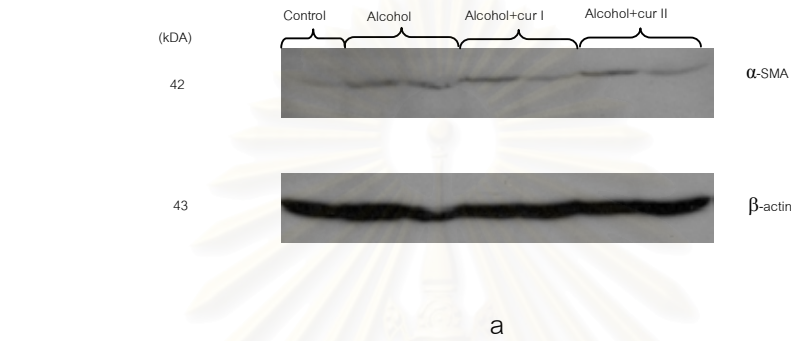

a

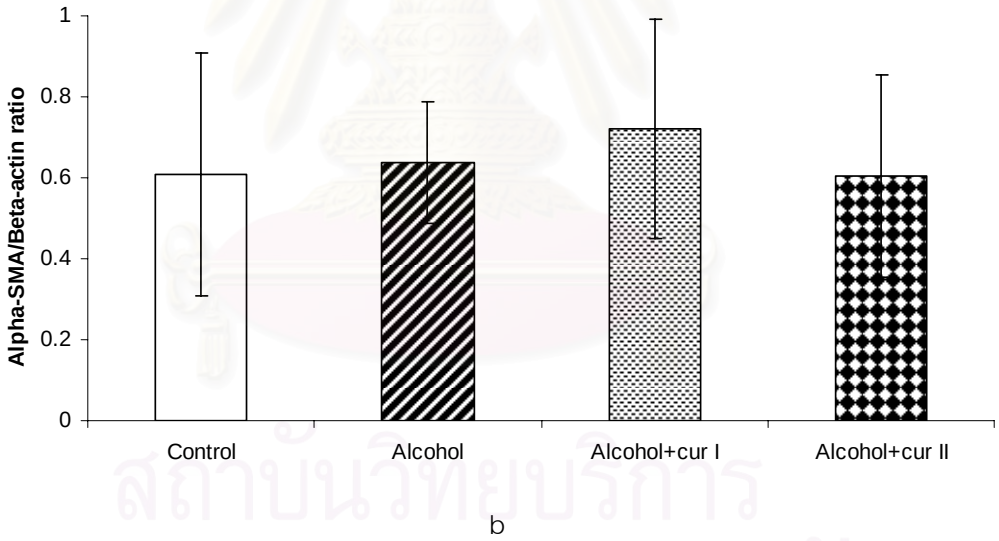

b

Figure 4-33. Representative blot of α-SMA expression (a) and the ratio to β-actin in all groups (b) (mean±SD)

CHAPTER V

DISCUSSION AND CONCLUSION

The present study found that the liver pathology in Alcohol group revealed mild to moderate steatosis, and mild necroinflammation as well as increased hepatic MDA, hepatocyte apoptosis and NF-κB activation. However, the results of SOD activity, PPARγ and □-SMA protein expression showed no difference among the groups. Curcumin treatments resulted in improving liver pathology, decreasing the elevation of hepatic MDA and NF-κB expression without improving hepatocyte apoptosis.

Effect of alcohol feeding on liver histopathology of rats

The pathological changes of ALD range from fatty liver to hepatic inflammation and necrosis (alcoholic hepatitis) to progressive fibrosis (alcoholic cirrhosis) (Tome and Lucey, 2004). In the present study, the livers in Alcohol group showed fatty change, necrosis and inflammation. Such histopathologic features typically represent alcoholic hepatitis.

A limitation of ALD model in this study was deserved discussion. It had to consider important genetic characteristics that rat differ from human including: 1) natural aversion to alcohol seen in general; 2) higher alcohol metabolic rate; 3) greater tolerance to alcohol (Tsukamoto et al., 1990). Therefore, rat rarely revealed the advanced stage of ALD. In addition, achieving alcohol consumption with high blood alcohol level was important to induce progressive alcoholic liver injury. For instance, oral liquid diets and intragastric alcohol feeding model can provide alcohol intake of 12 to 15 g/kg/day in rat that revealed high blood alcohol level (Ramaiah et al., 2004). Oral alcohol feeding in the present study could receive lower blood alcohol level than those models. Thus, the histopathologic features exhibited early stage of ALD (fatty liver and mild necroinflammation).

There have been reported that polyunsaturated fatty acids enriched in fish or corn oil promoted alcoholic liver injury and pathological changes in rats fed with alcohol containing polyunsaturated fatty acids (Polavarapu et al., 1998 and Nanji et al., 1999). In

many experiments, corn oil, fat used to supply energy composition of the animal diet, had no significant effect on liver pathology in control rats (Nanji et al., 1994 and 1999, Rouach et al., 1997 and Enomoto et al., 1999). Scientific evidence has shown that gender made a difference in alcohol-induced liver injury (Iimuro et al., 1997, Kono et al., 2000 and Yin et al., 2000). Females are more susceptible to alcohol-induced liver injury because: 1) gastric ADH-dependent alcohol metabolism is lower, resulting in higher blood alcohol levels; 2) plasma endotoxin levels are higher after alcohol ingestion; 3) the inflammatory response in the liver is more severe due to an estrogen-dependent sensitization to endotoxin (Moshage, 2001). To enhance the effect of alcohol, the present study employed female rats and used corn oil to provide calories of fat. In Alcohol group, body weight at the end of the experiment was lower than Control group. This result was similar to other previous studies (Yang et al., 2004 and Tipoe et al., 2008). A decrease of food intake would result in weight loss in Alcohol group; however, the condition of the animals remained good throughout the experiment.

Effect of alcohol feeding induced oxidative stress in rats

Alcohol oxidation generates toxic metabolites, free radicals and induces a state of oxidative stress which contributes to the pathogenesis of ALD. Importantly, oxidation of alcohol through the CYP 2E1 generates O_2^- and H_2O_2 (Das and Vasudevan, 2007, Brenner and Sigmund, 2004, Lieber, 1999). These free radicals are capable of damaging many cellular components such as DNA, protein and lipid (Gate, 1999). One of the characteristic features of oxidative stress is enhancement of lipid peroxidation. A number of experimental studies have demonstrated that alcohol intake increased the formation of lipid peroxidation product, such as MDA (Rouach et al., 1997, Polavarapu et al., 1998, Meagher, 1999). We found an increase in hepatic MDA level as well as pathological liver injury (fatty liver, necrosis and inflammation) in Alcohol group.

In addition, oxidative stress can injure liver cells directly by triggering apoptosis. Alcohol-induced liver injury has been linked to oxidative stress caused by the production of reactive oxygen intermediates that cause mitochondrial dysfunction, leading to a release of pro-apoptotic factors such as cytochrome C that can activate caspases and initiate the apoptotic cascade in hepatocytes (Natori et al., 2001). Jin and co-worker

observed the pathological changes and investigated the correlation of hepatocyte apoptosis with CYP2E1 expression and oxygen free radical in rats with ALD (Jin et al., 2007). Using the TUNEL assay, we detected a difference in apoptosis between the Control and Alcohol group that was similar to human alcoholic hepatitis and experimental rat model of ALD (Natori et al., 2001, Deaciuc, et al., 2003, Colantoni et al., 2003, Jin et al., 2007). The induction of CYP2E1 by alcohol feeding occurred in centrilobular area that extended to the midzonal area (Cohen et al., 1997, Tsutsumi et al., 1989). Our study showed that alcohol-induced hepatocyte apoptosis is predominantly distributed in the centrilobular area that suggested a causal link.

As described above, alcohol oxidation induced oxidative stress. To counteract this oxidative stress, cells have a variety of antioxidant enzymes, including SOD, catalase, and glutathione peroxidase. SOD catalyzes the rapid removal of O_2^- (Chaudier and Ferrari-Iliou, 1999). The effects of chronic alcohol exposure on activity of SOD are controversial, with reports of decrease (Jin et al., 2007, Polavarapu et al., 1998) or no change (Yang et al., 2004, Li et al., 2004). These studies may reflect variations in experimental design, diet, and duration of alcohol feeding. Decreased SOD activity in alcohol fed rats was associated with enhance of lipid peroxidation and severe pathology of liver (Polavarapu et al., 1998). Rats fed with alcohol and fish oil showed the most severe pathologic changes, the highest level of lipid peroxidation and decreased of CuZn-SOD activity, whereas only alcohol administration did not decrease CuZn-SOD activity in groups showed the lower level of lipid peroxidation, and had no necroinflammatory change. Our model showed the slight increase of MDA level, no change of SOD activity and mild histopathology changes for steatosis and necroinflammation. This data might reflect that the slight increase of MDA level did not significantly inactivate SOD.

Effect of alcohol feeding induced liver NF-κB activation in rats

Alcohol administration induces oxidative stress that initiates or amplifies inflammation through up-regulation of several genes involved in the inflammatory response. One such gene is NF-κB, whose activation results in the up-regulation of proinflammatory cytokines, such as TNF-□, IL-1, chemokines and adhesion molecules

(Pahl, 1999). Activation of NF-κB and upregulation of cytokine production occurred in alcoholic liver injury and were associated with lipid peroxidation (Nanji et al., 1999 and 2003, Jokelainen et al., 2001). Using the immunohistochemical technique, the present study found positive staining in nuclei of hepatocytes in Alcohol group suggesting an induction of NF-κB activation in rat model of ALD.

Effect of alcohol feeding on liver PPARγ expression in rats

PPARγ is a nuclear transcription factor activated by specific ligands. It appeared to be related to the inflammation and liver fibrosis (Kon et al., 2002, Zhao et al., 2004). For example, pioglitazone, the ligand of PPARγ could prevent liver from inflammation, necrosis and increase of TNF-□ caused by CCl_4 (Kon et al., 2002). Decreased PPARγ expression has been found to associate with HSC activation and treatment of cultured activated HSC with PPARγ ligands inhibited the expression of □-SMA and type I precollagen (Miyahara et al., 2000). More recently, a decrease of PPARγ expression was found in alcoholic liver fibrosis rats (Zhao et al., 2004). Rats fed alcohol with high fat diet presented fatty change, inflammation and fibrosis in the liver. This stage showed severe liver injury and HSC activation. As HSCs undergo a process known as activation, cytokines and growth factor are upregulated. Platelet-derived growth factor when being expressed is capable of inhibiting PPARγ expression via mitogen-activated protein kinase-mediated phosphorylation of PPARγ (Galli et al., 2003). Also, TNF-α , inflammatory cytokine, is known to inhibit PPARγ expression in adipocytes and HSC activation in liver fibrosis (Tanaka et al., 1999 and Miyahara et al., 2000). Thus alcoholic liver fibrosis rats could decrease PPARγ expression. Our model showed only mild steatosis, necroinflammation and no change of □-SMA protein expression indicating that there was no HSC activation. Although, in this present study, PPARγ protein expression did not increase significantly in Alcohol group, PPARγ might have a tendency to be induced in rats with alcoholic hepatitis. However, it remained unclear how PPARγ expresses in different stages of ALD. Further studies are required to elucidate the role of PPARγ on pathophysiology of ALD.

Antioxidant effect of curcumin in rats with alcoholic hepatitis

Curcumin, is the active ingredient isolated from the rhizomes of the plant *Curcuma longa* Linn. It is known to have an antioxidant property. In this study, curcumin was used at either 200 or 600 mg/kg BW per dose. Because of rapid metabolism of curcumin, rats were fed curcumin twice a day. So, the rats received a total amount of curcumin at either 400 or 1,200 mg/kg BW a day, respectively. In addition, there was no significant difference in body weight in curcumin treatment groups at the end of the experiment.

Curcumin is the free radical scavenger and inhibited lipid peroxidation product. *In vitro* study, curcumin scavenged O_2^-, H_2O_2 and nitrite radical from activated macrophage (Joe and Lokesh, 1994). For *in vivo* study, it has been reported to inhibit CCl_4-initiate lipid peroxidation product (Akia et al., 1998, Park et al., 2000). The present study also indicated that curcumin treatments decreased level of MDA (marker of oxidative stress) as well as improved liver pathology. It was conceivable that curcumin could protect against the free radical mediated oxidative stress by scavenging of free radicals in rats with alcoholic hepatitis.

The recent study, Ghoneium found the effects of curcumin on acute alcohol-induced apoptosis using suspension and monolayer cultures of isolated hepatocytes (Ghoneium, 2009). Curcumin concentrations of 0.1-10 mM diminished the alcohol-induced lipid peroxidation. In addition, 1 μM of curcumin decreased cytochrome C translocation in hepatocyte monolayers whereas 10 mM of curcumin induced caspase-3 activation and apoptosis. This data indicated that low concentration of curcumin may protect hepatocytes by reducing lipid peroxidation and cytochrome C release. Conversely, higher concentration of curcumin provoked caspase-3 activation and hepatocytotoxicity *in vitro* model (Ghoneium, 2009). The present study found a significant reduction of MDA level in curcumin treatments. The hepatocyte apoptosis might have a tendency to decrease in low dose of curcumin treatment. In contrast, high dose of curcumin treatment had an increase apoptosis compared to Control. The present study could indicate that high dose of curcumin might have apoptotic effect on hepatocytes, however more experiments are needed to evaluate the apoptotic effect of curcumin in ALD model.

Anti-inflammatory effect of curcumin in rats with alcoholic hepatitis

According to NF-κB involving inflammation, NF-κB has been showed to be inhibited by curcumin *in vitro* and *in vivo* studies. Curcumin has been observed to suppress TNF-□ induced NF-κB activation in human myeloid ML-1a cells (Singh and Aggarwal, 1995). The data exhibited that curcumin can directly inhibit NF-κB activation. Reyes-Gordillo and co-workers also reported that curcumin was able to avoid NF-κB translocation to the nucleus induced by CCl_4 administration as a result of decreased inflammatory cytokines such as TNF-α IL-1β (Reyes-Gordillo et al., 2007). For ALD model, it has been reported that curcumin prevented NF-κB binding activity and inhibited the expression of NF-κB-dependent genes (Nanji et al, 2003). The present study showed that curcumin decreased the number of NF-κB positive cells in rats with alcoholic hepatitis that agreed with the previous study (Nanji et al, 2003). Curcumin could block many steps that activate NF-κB. For example, curcumin inhibited the step before the phosphorylation and subsequent release of IκB complexed to NF-κB (Singh and Aggarwal, 1995). Next, curcumin prevented phosphorylation of IκB by inhibiting the activity of IKK (Jobin et al., 1999, plummer et al., 1999). Brennan and O'Neill (1998) found that curcumin inhibited NF-κB by interfering with IκBα degradation and reacts with p50 in the NF-κB complex.

The present study also revealed more improvement of necroinflammation score in low dose of curcumin treatment than high dose while the reduction of NF-κB expression was exhibited similarly between two doses of curcumin treatment. This could be explained that another pathway(s) may induce inflammation response that indirectly mediated by NF-κB.

Recent data have shown that the anti-inflammatory effect of curcumin in an experimental model of sepsis is mediated by up-regulation of PPARγ and another study activated PPARγ with curcumin could interfere NF-κB activity and increase PPARγ expression in HSCs (Xu et al., 2003). These data suggested that PPARγ activation could relate to the inflammation and liver fibrosis. Because of no change in PPARγ protein expression in Alcohol group, the study could not determine the anti-inflammatory effect of curcumin mediated by PPARγ pathway.

Curcumin has an antioxidant property. It could prevent free radical mediated oxidative stress and consequently inhibited NF-κB activation. This study indicated that curcumin could attenuate inflammation through reduction of oxidative stress and inhibition of NF-κB activation.

In conclusion, the study found that curcumin could attenuate liver injury induced by alcohol through the reduction of oxidative stress and inhibition of NF-κB activation. While curcumin might have a tendency to decrease hepatocyte apoptosis, PPARγ protein expression did not change in early stage of alcohol-induced liver injury. Thus, the effect of curcumin on PPARγ protein expression in rats with alcoholic hepatitis could not be determined in this study.

REFERENCES

English

Akila, G., Rajakrishnan, V., Viswanathan, P., Rajashekaran, K.N., and Menon, V.P. Effects of curcumin on lipid profile and lipid peroxidation status in experimental hepatic fibrosis. Hepatol Res 11(1998) : 147-157.

Arora, R., Basu, N., and Kapoor, V. Anti-inflammatory studies on *Curcuma longa* (tumeric). Indian J Med Res 59(1971) : 1289-1295.

Bellentani, S., et al. Prevalance of chronic liver disease in the general population of northern Italy: the Dionysos Study. Hepatology 20(1994) : 1442-1449.

Betteridge, D.J. What is oxidative stress? Metabolism 49(2000) : 3-8.

Boveris, A., Oshino, N., and Chance, B. The cellular production of hydrogen peroxide. Biochem J 128(1972) : 617-630.

Brennan, P., and O'Neil,l L.A. Inhibition of nuclear factor kappaB by direct modification in whole cells-mechanism of action of nordihydroguaiaritic acid, curcumin, and thiol modifiers. Biochem Pharmacol 55(1998) : 965-973.

Brenner, D.A., and Sigmund, S. Pathogenesis of alcoholic hepatitis. J Gastroenterol Hepatol 19(2004) : S229-S235.

Brouet, I., and Ohshima, H. Curcumin, anti-tumour promoter and anti-inflammatory agent, inhibits induction of nitric oxide synthase in activated macrophages. Biochem Biophys Res Commun 206(1995) : 533-540.

Carpino, G., et al. Alpha-SMA expression in hepatic stellate cells and quantitative analysis of hepatic fibrosis in cirrhosis and in recurrent chronic hepatitis after liver transplantation. Dig Liver Dis 37(2005) : 349-356.

Chan, M.M. Inhibition of tumor necrosis factor by curcumin, a phytochemical. Biochem Pharmacol 49(1995) : 1551-1556.

Chaudier, J., and Ferrari-Iliou R. Intracellular antioxidants: from chemical to biochemical mechanisms. Food Chem Toxicol 37(1999) : 949-62.

Cheng, A.L., et al. Phase I clinical trial of curcumin, a chemopreventive agent, in patients with high-risk or pre-malignant lesions. Anticancer Res 21(2001) : 2895-2900.

Cohen P.A., et al. Immunohistochemical determination of hepatic cytochrome P-4502E1 in formalin-fixed, paraffin-embedded sections. Alcohol Clin Exp Res 21(1997) : 1057-1062.

Colantoni, A., Idilman, R., Maria, N.D., Paglia, N.L., Belmonte, J., Wezeman, F., et al. Hepatic apoptosis and proliferation in male and female rats fed alcohol: role of cytokines. Alcohol Clin Exp Res 27(2003) : 1184-1189.

Das, S.K., and Vasudevan, D.M. Alcohol-induced oxidative stress. Life Sci 81(2007) : 177-187.

Deaciuc I.V., et al. Inhibition of caspases in vivo protects the rat liver against alcohol-induced sensitization to bacterial lipoplysaccharide. Alcohol Clin Exp Res 25(June 2003) : 935-943.

Debril, B.M., Renaud, J.P., Fajas, L., and Auwerx, J. The pleiotropic functions of peroxisome proliferator-activated receptorγ. J Mol Med 79(November 2001) : 30–47.

Diehl, A.M. Nonalcoholic steatohepatitis. Semin Liver Dis 19(1999) : 221-229.

Enomoto, N., Yamashina, S., and Kono, H . Development of new, simple model of early alcohol-induced liver injury based on sensitization of Kupffer cells. Hepathology 29(1999) : 1680-1689.

Enomoto, N., et al. Prevention of ethanol-induced liver injury in rats by an agonist of peroxisome proliferator-activated receptor-γ, pioglitazone. J Pharmacol Exp Ther. 306(2003) : 3846–3854.

Faremi, T.Y., Suru, S.M., Fafunso, M.A., Obioha U.E. Hepatoprotective potentials of Phyllanthus amarus against ethanol-induced oxidative stress in rats. Food Chem Toxicol 46(2008) : 2658–2664

Gate, L., Paul, J., Ba, N., Tew, K.D., and Tapiero, H. Oxidative stress induced in pathologies: the role of antioxidants. Biomed Pharmacother 53(1999) : 169-180.

Galli, A., Crabb, D., and Price, D. Peroxisome proliferator-activated receptorγ transcriptional regulation is involved in platelet-derived growth factor-induced proliferation of human hepatic stellate cells. Hepatology. 31(2000) : 101-108.

Ghoneim, A.I. Effects of curcumin on ethanol-induced hepatocyte necrosis and apoptosis: implication of lipid peroxidation and cytochrome C. Naunyn-schmiedeberg's Arch Pharmacol. 379(2009) : 47-60.

Gilmore, T.D. The Rel/NF-kB signal transduction pathway: introduction. Oncogene 18(1999) : 6842-6844.

Gramenzi, A., et al. Review article: alcoholic liver disease-pathophysiological aspects and risk factors. Aliment Pharmacol Ther 24(2006) : 1151-1161.

Grimm, S., and Baeuerle, P.A. The inducible transcription factor NF-κB : structure-function relationship of its protein subunits. Biochem J 290(1993) : 297–308.

Gupta, B., and Ghosh, B. Curcuma longa inhibits TNF-alpha induced expression of adhesion molecules on human umbilical vein endothelial cells. Int J Immunopharmacol 21(1999) : 745–757.

Hall, P.M. Pathological spectrum of alcoholic liver disease. In Hall, P. (ed), Alcoholic liver disease. Pp. 41-70. London: Edward Arnold,1995.

Halliwell, B. Antioxidants and human disease: A general introduction. Nutr Rev 55(1997) : S44-S49.

Halliwell, B., and Gutteride, J. M. Oxygen toxicity, oxygen radicals, transition metals and disease. Biochem J 219(1984) : 1-14.

Iimuro, Y., Frankenberg, M.V., Arteel, G.E., Bradford, B.U., Wall, C.A., and Thurman, R.G. Female rats exhibit greater susceptibility to early alcohol-induced liver injury than males. Am J Physiol Gastrointest Liver Physiol 272(1997) : G1186-G1194.

Ireson, C., et al. Characterization of metabolites of the chemopreventive agent curcumin in human and rat hepatocytes and in the rat in vivo, and evalution of their ability to inhibit phorbol ester-induced prostaglandin E2 production. Cancer Res 61(2001) : 1058-1064.

Janero, D.R. Malondialdehyde and thiobarbituric acid-reactivity as diagnostic indices of lipid peroxidation and peroxidative tissue injury. Free Radic Biol Med 9(1990) : 515-540.

Ji, L.L., and Hollander, J. Antioxidant defense: effects of aging and exercise. Radak, Z (ed), Free Radicals in exercise and aging, p.38. Illinois: Human Kinetics, 2000.

Jin, W.P., Quan, X.Q., Menq, F.P., Cui, X.D., and Piao, H.J. Relationship among hepatocyte apoptosis, P450 2E1 and oxidative stress in alcoholic liver disease of rats. Zhongguo Wei Zhong Bing Ji Jiu Yi Xue 19(2007) : 419-421.

Jobin, C. et al. Curcumin blocks cytokine-mediated NF-kappa B activation and proinflammatory gene expression by inhibiting inhibitory factor I-kappa B kinase activity. J Immunol 163(1999) : 3474-3483.

Joe, B., and Lokesh BR. Role of capsaicin, curcumin and dietary n-3fatty acids in lowering the generaton of reactive oxygen species in rat peritoneal macrophages. Biochim Biophys Acta 1224(1994) : 255-263.

Jokelainen, K., Lester, A., Amin, A., Nanji, A.A. NF-κB activation is associated with free radical generation and endotoxemia and precedes pathological liver injury in experimental alcoholic liver disease. Cytokine 16(October 2001) : 36-9.

Kon, K., et al. Piogliitazone prevents early-phase hepatitic fibrogenesis caused by carbon tetrachloride. Biochem Biophys Res Commun 291(2002) : 55-61.

Kono, H., et al. Gender differences in early alcohol-induced liver injury: role of CD14, NF-κB and TNF-α. Am J Physiol 278(2000) : G652-G661.

Li, Y., Chen, S., Yu, C., Zhang, Y., and Xu, G. Effect of acute alcoholism on hepatic enzymes and oxidation/antioxidation in rats. Hepatobiliary Pancreat Dis Int 3(May 2004) : 241-244.

Lieber, C.S. Microsomal ethanol-oxidizing system (MEOD): the first 30 years (1968-1998)-a review. Alcohol Clin Exp Res 23(June 1999) : 991-1002.

Lieber, C.S., and Decarli, L.M. Liquid diet technique of ethanol administration:1989 update. Alcohol Alcoholism 24(1989) : 197–211.

Lowry, O.H., Rosebrough, N.J., and Farr, A.L. Protein measurement with the folin phenol reagent. J Biol Chem 193(1951) : 265-275.

MacSween, R.N., and Burt, A.D. Histologic spectrum of alcoholic liver disease. Semin Liver Dis 6(1986) : 221-232.

Meagher, E.A., Barry, O.P., Burke, A., Lucey, M.R., Lawson, J.A., Rokach, J., et al. Alcohol-induced generation of lipid peroxidation products in humans. J Clin Invest 104(1999) : 805-813.

Miyahara, T., et al. Peroxisome proliferators-activated receptors and hepatic stellate cell activation. J Biol Chem 275(2000) : 35715–35722.

Moraes, L.A., Piqueras, L., and Bishop-Bailey, D. Peroxisome proliferator-activated receptors and inflammation. Pharmacol Ther 110(2006) : 371– 385.

Moreno, A., and Pares, X. Purification and characterization of a new alcohol dehydrogenase from human stomach. J Biol Chem 266(1991) : 1128-1133.

Moshage, H. Alcoholic liver disease: a matter of hormones? J Hepatol 35(2001) : 130-133.

Nanji, A.A., et al. Nitric oxide production in experimental alcoholic liver disease in the rat: role in protection from injury. Gastroenterology 109(1995) : 899–907.

Nanji, A,A,, et al. Enhanced cyclooxygenase-2 gene expression in alcoholic liver disease in the rat. Gastroenterology 112(1997) : 943–951.

Nanji, A.A., et al. Activation of Nuclear factor kappa B and cytokine inbalance in experimental alcoholic liver disease in the rat. Hepatology 30(1999) : 933-943.

Nanji, A.A., Jokelainen, K., Tipoe, G.L., Rahemtulla, A., Thomas, P., Dannenberg, A.J. Curcumin prevents alcoholinduced liver disease in rats by inhibiting the expression of NF-kappa B-dependent genes. Gastrointest Liver Physiol 284(2003) : G321-G327.

Nanji, A.A., Khwaja, S., Tahan, S.R., and Sadrzadeh, S.M.H. Plasma levels of a novel noncyclooxygenase-derived prostanoid (8-isoprostane) correlate with severity of liver injury in experimental alcoholic liver disease. J Pharmacol Exp Ther 269(1994) : 1280-1285.

Nanji, A.A., Zhao, S., Sadrzadeh, S.M.H., and Waxman, D.J. Use of reverse transcriptase-polymerase chain reaction to evaluate invivo cytokine gene expression in rats fed ethanol for long periods. Hepatology 19(1994) : 1483–1487.

Natori, S., Rust, C., Stadheim, L.M., Srinivasan, A., Burgart, L.J., and Gores, G. Hepatocyte apoptosis is a pathologic feature of human alcoholic hepatitis. J Hepatol 34(2001) : 248-253.

Nouchi, T., Tanaka, Y., Tsukada, T., Sato, C., and Marumo, F. Appearance of alpha-smooth-muscle-actin-positive cell in hepatic fibrosis. Liver 11(1991) : 100-105.

Ohata, M., et al. Pioglitazone prevents acute liver injury induced by ethanol and lipopolysaccharide through the suppression of tumor Necrosis Factor-α. Alcohol Clin Exp Res 28(August 2004) : 139S-144S.

Ohgawa, H., Ohishi, N., and Yagi, K. Assay for lipid peroxides in animal tissues by thiobarbituric acid reaction. Anal Biochem 95(1979) : 351-358.

Ozaras, R., Tahan, V., Aydin, S., Uzun, H., Kaya, S., and Senturk, H. N-acetylcysteine attenuates alcohol-induced oxidative stess in rats. World J Gastroenterol 9(April 2003) :791-794.

Pageaux, G.P., Bismuth, M., and Perney, P. Alcohol relapse after liver transplantion for alcoholic liver disease: dose it matter? J Hepatol 38(2003) : 629-634.

Pahl, H.L. Activators and target genes of Rel/NF-κB transcription factors. Oncogene 18(1999) : 6853-6866.

Pan, M.H., Huang, T.M., and Lin, J.K. Biotransformation of curcumin through reduction and glucuronidation in mice. Drug Metab Dispos 27(1999) : 486-494.

Park, E.J., Jeon, C.H., KO, G., Kim, J., Sohn, D.H. Protective effect of curcumin in rat liver injury induced by carbon tetrachloride. J Pharm Pharmacol 52(2000) : 437-440.

Plummer, S.M., et al. Inhibition of cyclo-oxygenase 2 expression in colon cells by the chemopreventive agent curcumin involves inhibition of NF-kappa B activation via the NIK/IKK signaling complex. Oncogene 18(1999) : 6013-6020.

Polavarapu, R., et al. Increased lipid peroxidation and impaired antioxidant enzyme function is associated with pathological liver injury in experimental alcoholic liver disease in rats fed diets high in corn oil and fish oil. Hepatology 27(1998) : 1317-23.

Ramaiah, S.K., Rivera, C., and Arteel, G.E. Early-phase alcoholic liver disease: an update on animal models, pathology, and pathogenesis. Int J Toxicol 23(2004) : 217-231.

Ravindranath, V., and Chandrasekhara, N. Absorption and tissue distribution of curcumin in rats. Toxicology 16(1980) : 259-265.

Ravindranath, V., and Chandrasekhara, N. Metabolism of curcumin-studies with [^{3}H] curcumin. Toxicology 16(1982) : 259-265.

Reddy, A.C., and Lokesh, B.R. Effect of dietary turmeric (Curcuma long) on iron-induced lipid peroxidation in rat liver. Food Chem Toxicol 32(1994) : 279-283.

Reddy, A.C., and Lokesh, B.R. Effect of curcumin and eugenol on iron-induced hepatic toxicity in rats. Toxicology 107(1996) : 39-45.

Reyes-Gordillo, K., Segovia, J., Shibayama, M., Vergara, P., Moreno, MG., and Muriel, P. Curcumin protects against acute liver damage in the rat by inhibiting NF-κB, proinflammatory cytokines production and oxidative stress. Biochimica et Biophysica Acta 1770(2007) : 989-996.

Ricole, M., Li, A.C., Willson, T.M., Kelly, C.J., and Glass, C.K. The peroxisome proliferator-activated receptor γ is a negative regulator of macrophage activation. Nature 391(1998) : 79-82.

Reppaport, A. M. Anatomic considerations. 4th ed. pp. 1-49. Philadelphia, 1956.

Roizen, R., Kerr, W.C., and Fillmore, K.M. Cirrhosis mortality and per capita consumption of distilled spirits, United States, 1949-1994: trend analysis. BMJ 319(1999) : 666-670.

Romanes, G. J. Cunningham's mannual of practical anatomy. Volume two thorax and abdomen. 15th ed. pp.115. The United States: Oxford Medical Publications,1986.

Ronis, M.J.J., et al. Effects of N-acetylcysteine on ethanol-induced hepatotoxicity in rats fed via total enteral nutrition. Free Radic Biol Med 39(2005) : 619-630

Ross, M. H., Kaye G. I., and Pawlina, W. Histology: A text and atlas. 4th ed. pp. 535-539. The United States: Lippincott Williams & Wilkins, 2003.

Rouach, H., Fataccioli, V., Gentil, M., French, SW., Morimoto, M., and Nordmann R. Effect of chronic ethanol feeding on lipid peroxidation and protein oxidation in relation to liver pathology. Hepatology 25(1997) : 351-355.

Safdar, K., and Schiff, E.R. Alcohol and hepatitis C. Semin Liver Dis 55(2004) : 965-973.

Shapiro, H., Ashkenazi, M., Weizman, Nir., Shahmurov, M., Aeed, H., and Bruck, R. Curcumin ameliorates acute thioacetamide-induced hepatotoxicity. J Gastroenterol Hepatol 21(2006) : 358-366.

Sies, H. Oxidative stress: oxidants and antioxidants. Exp Physiol 82(1997) : 291-295.

Singh, S., and Aggarwal, B.B. Activation of transcription factor NF-kapp B is suppressed by curcumin (diferuloylmethane). J Biol Chem 270(1995) : 24995-25000.

Skalli O, Ropraz P, Trzeciak A, Benzonana G, Gabbiani G. A monoclonal antibody against alpha-smooth muscle actin: a new probe for smooth muscle differentiation. Cell Biol 103(1986) : 2787-2796.

Sørensen, T.I., Orholm, M., Bentsen, K.D., Hoybye, G., Eghoje, K., and Christoffersen, P. Prospective evaluation of alcohol abuse and alcoholic liver injury in men as predictors of development of cirrhosis. Lancet 2(1984) : 241-244

Sreejayan, N., and Rao, M.N. Free radical scarvenging activity of curcuminoids. Arzneimittelforschung. 46(1996) : 169-171.

Sreejayan, N., and Rao, M.N. Nitric oxide scavenging by curcuminoids. J Pharm Pharmacol. 49(1997) : 105-107.

Stewart, S.F., and Day C.P. Alcoholic liver disease. In Boyer T.D., Wright T.L., and Manns M.P. (eds.), Zakim and Boyer's Hepatology A Textbook of Liver Disease. 5th ed. pp. 579-582. Canada: Saunders Elsevier, 2006.

Tanaka, T., et al. Down regulation of peroxisome proliferator-activated receptor γ expression by inflammatory cytokines and its reversal by thiazolidinediones. Diabetologia 42(1999) : 702-710.

Takano, H., et al. Peroxisome proliferator–activated receptor activators inhibit lipopolysaccharide-induced tumor necrosis factor α expression in neonatal rat cardiac myocytes. Circ Res. 29(September 2000) : 596-602.

Tipoe, G.L., Liong, E.C., Casey, C.A., Donohue Jr, T.M., Eagon, P.K., and So, H. A voluntary oral ethanol-feeding rat model associated with necroinammatory liver injury. Alcohol Clin Exp Res 32(April 2008) : 669-682.

Tome, S., and Lucey, M.R. Review article: current management of alcoholic liver disease. Aliment Pharmacol Ther 19(2004) : 707-714.

Tortora, G. J., and Grabowski, S. R. Principles of anatomy and physiology. 9th ed. pp. 843-845. The United States: John Witey & Sons, 2000.

Towbin, H., Staehelin, T., and Gordon, J. Electrophoretic transfer of proteins from polyacrylamide gels to nitrocellulose sheets: procedure and some applications. P. Natl. Acad. Sci. USA. 76(1979) : 4350-4354.

Tsukamoto, H., Gaal, K., and French, S.W. Insights into the pathogenesis of alcoholic liver necrosis and fibrosis: status report. Hepatology. 12(1990) : 599-608.

Tsukamoto, H., Towner, S.J., Cifalo, L.M., and French, S.W. Ethanol-induced liver fibrosis in rats fed high-fat diet. Hepatology 6(1986) : 814–822.

Tsutsumi, M., Lasker, J.M., Shimizu, M., Rosman, A.S., and Lieber, C.S. The intralobular distribution of ethanol-induced P450IIEI in rat and human. Hepatology 10(1989) : 437-446.

Uzun, H., et al. Potential effects of L-NAME on alcohol-induced oxidative stress. World J Gastroenterol 11(January 2005) : 600-604

Wahltrom, B., and Blennow, G. A study on the fate of curcumin in the rat. Pharmacol Toxicol 43(1978) : 86-92.

Winterbourn, C.C., Hawkins, R.E., Brian, M., and Carrell, R.W. The estimation of red cell superoxide dismutase activity. J Lab Clin Med 85(1975) : 337-341.

Wu, D., and Cederbaum, A.I. Alcohol, oxidative stress, and free radical damage. Alcohol Res Health 27(2003) : 277-84.

Xu, H., Fu, Y., and Chen, A. Activation of peroxisome proliferator-activated receptor-γ contributes to the inhibitory effects of curcumin on rat hepatic stellate cell growth. Am J Physiol Gastrointest Liver Physiol 285(2003) : G20-G30.

Yang, S., Huang, C., Chu, J., and Chen, J. Effects of β-carotene on cell viability and antioxidant status of hepatocytes from chronically ethanol-fed rats. Br J Nutr 92(2004) : 209-215.

Yin, M., et al. Estrogen is involved in early alcohol-induced liver injury in a rat enteral feeding model. Hepatology 31(2000) : 117-123.

Yuan, G., Zhou, X., Gong, Z., Zhang, P., Sun, X., and Zheng, S. Expression and activity of inducible nitric oxide synthase and endothelial nitric oxide synthase correlate with ethanol-induced liver injury. World J Gastroennterol 12(April 2006) : 2375-81.

Zhao, C.Y., Jiang, L.L., Li, L., Deng, Z.J., Liang, B.L., and Li, J.M. Peroxisome proliferator-activated receptor-γ in pathogenesis of experimental fatty liver disease. World J Gastroenterol. 10(May 2004) : 1329-1332.

Zingarelli, B., Sheehan, M., Hake, P.W., Connor, M., Denenberg, A., and Cook, J.A. Peroxisome proliferator activator receptor-γ ligands, 15-Deoxy-$\Delta^{12,14}$-prostaglandin J_2 and ciglitazone, reduce systemic inflammation in polymicrobial

sepsis by modulation of signal transduction pathways. J Immunol. 171(2003) : 6827–6837.

http://www.biomed.metu.edu.tr/courses/term_papers/bioartf-liver_kenar.htm [2009, March 6]

http://www.genmall.com.tw/products/INFO/Bulletin_2134B%20Increased%20Transfer%20Efficiency%20Using%20a%20Discontinuous%20Buffer%20System%20With%20the%20Trans-Blot%20SD%20Cell%20Rev%20B.pdf [2009, March 7]

http://www.hoeferinc.com/downloads/SE260-IM.pdf [2009, March 7]

http://www.ics.trieste.it/MAPs/MedicinalPlants_Plant.aspx?id=605 [2009, March 8]

http://www.kumc.edu/instruction/medicine/anatomy/histoweb/path/path03.htm [2009, March 7]

http://www.medscape.com/content/2004/00/48/89/488939/488939_fig.html [2009, March 7]

http://www.pathology.med.umich.edu/greensonlab/etoh-fat.jpg [2009, March 7]

APPENDICES

APPENDIX A

Study of ALD Model in This Thesis

1. Introduction

The use of a variety of animal models in the study of ALD reflects the task of developing a suitable model that replicates the human prototype (Lieber et al., 1989). In 1989, Lieber and co-workers developed oral liquid diets (Lieber-DeCarli Diets) that contained 35.5% energy from alcohol. They observed only steatosis, no inflammation and fibrosis. Alcohol containing liquid diets and alcohol feeding via surgically implanted gastrostomy tubes (Tsukamoto-French model) have used to overcome these problems and have produced liver injury in the rat (Tsukamoto et al., 1986). This model was expensive, requirements and constant animal monitoring. More recently, Enomoto and colleagues (1999) reported a new rat model in which female wistar rats received 5 g/kg alcohol intragastrically every 24 hours. After 4 weeks, this treatment induced fat accumulation, inflammation, and necrosis in the liver (Enomoto et al., 1999). However, other researchers still must reproduce and confirm this model to establish its validity. Therefore, our objective was to establish a simplified and reliable animal model of ALD.

2. Materials and Methods

2.1 Animal Preparation

Male and Female Sprague-Dawley rats, weighing 180-220 g, were purchased from the National Laboratory Animal Center, Mahidol University, Salaya, Nakorn Pathom. The rats were kept in a controlled temperature room at 25±1 ^{o}C under standard conditions (12 hour day-night rhythm) and had freely access to food and tap water. All rats received well care in accordance with the Ethical Committee, Faculty of Medicine, Chulalongkorn University, Thailand.

2.2 Experimental Protocols

All rats were randomly divided into 5 experimental groups (2-3 rats/group).

Group 1-3: Male and female rats were fed orally with various doses of alcohol (5, 7, 7.5 g/kg BW a day) twice a day and received standard diet for 4, 8, 10, 14 and 24 weeks.

Group 4: Female rats were fed orally with alcohol (7.5 g/kg BW a day) and received custom-made diet which contained 35% of energy from fat, 18% from protein and 47% from carbohydrate (Enomoto et al., 1999) for 4 and 8 weeks

Group 5: Female rats were received only custom-made diet (Enomoto et al., 1999) for 4 and 8 weeks

All rats were weighed weekly. At the end of the study, they were sacrificed using intraperitoneal injection of an overdose of thiopental sodium. The abdominal wall was opened and the whole liver was removed. The liver was fixed in 10% formalin solution to determine histopathology.

All samples were evaluated by an experienced pathologist who is blinded to the experiment. All fields in each section were examined for grading of steatosis and necroinflammation according to Colantoni et al.'s criteria (Colantoni et al., 2003)

Steatosis was scored as the percentage of parenchymal cells containing fat (micro-or macrosteatosis).

0 = no parenchymal cells containing fat

1 = <20% of parenchymal cells containing fat

2 = 20–39% of parenchymal cells containing fat

3 = 40–50% of parenchymal cells containing fat

4 = >51% of parenchymal cells containing fat

Inflammation and necrosis were scored by the number of foci of inflammation and necrosis identified under low-power field of light microscope.

0 = no inflammation and necrosis

1 = 1 focus per low-power field of inflammation and necrosis

2 = 2 foci per low-power field of inflammation and necrosis

3 = 3 or more foci per low-power field of inflammation and necrosis

3. Results and Discussion

The histopathologic changes of rat liver were summarized in Table 2-2 and examples of liver histopathology were showed in Figure 2-14.

Group 1, 2 and 3 appeared normal histopathology both male and female at 4, 8, 10, 14 and 24 weeks. This experiment, 7.5 g/kg BW a day of alcohol was maximum dose that cause no death in rats. This dose is lower than liquid diet model that they used alcohol 14-18 g/kg BW (Lieber and Decarli, 1989). Our study indicated that only alcohol administration had limitation to develop ALD model.

Because gender difference and diet associates alcohol-induced liver injury (Iimuro et al., 1997, Kono et al., 2000, Yin et al., 2000, Polavarapu et al., 1998) next study female rats were used. Group 4 showed fatty change and mild necroinflammation at 4 weeks but no necroinflammation was found at 8 weeks. Only mild fatty change revealed in group 4 at 8 weeks. Moreover, only control diet (group 5) did not affect on liver histopathology. This data supported that role of dietary polyunsaturated fatty acid may potentiate in alcohol-induced liver injury. Thus, female Sprague-Dawley rats fed with alcohol 7.5 g/kg BW + custom diet (group 4 at 4 weeks) will be used for our future research study.

In conclusion, our study could establish a simplified and reliable animal model of ALD. This model can be useful for future research study.

Table 2-2. The histopathological changes in rats

Group	Sex	Histopathological changes in rat liver				
		4 weeks	8 weeks	10 weeks	14 weeks	24 weeks
1) Alcohol 5 g/kg BW	Male	-	Normal	-	-	Normal
	Female	-	Normal	-	-	-
2) Alcohol 7 g/kg BW	Male	-	-	Normal	Normal	-
	Female	-	-	-	-	Normal
3) Alcohol 7.5 g/kg BW	Male	Normal	Normal	-	-	-
	Female	Normal	Normal	-	-	-
4) Alcohol 7.5 g/kg BW +Custom diet	Female	Fatty change and mild necroinflammation	Fatty change	-	-	-
5) Custom diet	Female	Normal	Normal	-	-	-

Note: Custom-made diet contained 35% of energy from fat, 18% from protein and 47% from carbohydrate (Enomoto et al., 1999) and ingredients of diet were showed in Appendix B.

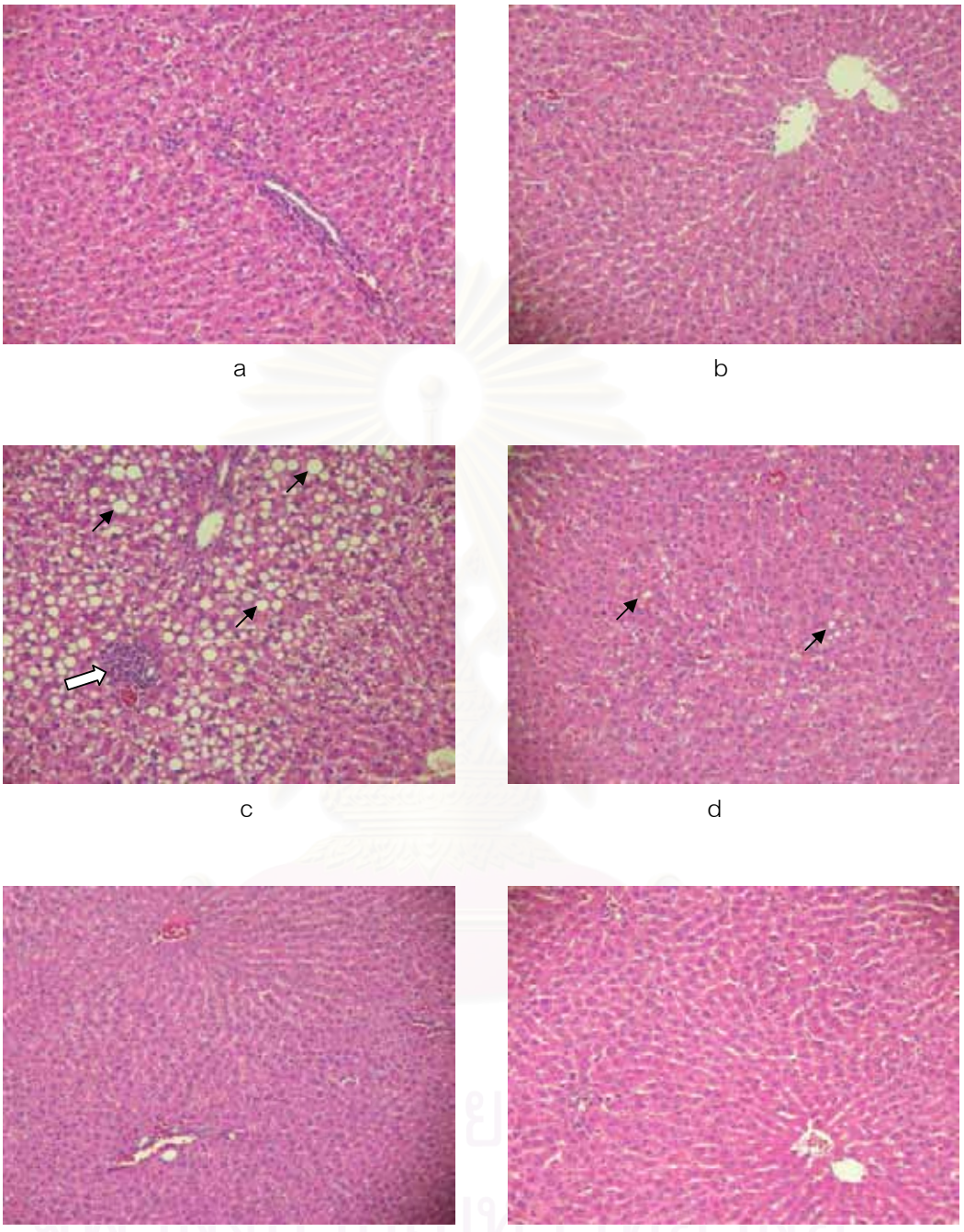

Figure 2-14. Hematoxylin-eosin stained liver sections (x400), a) group 1 (male at 24 weeks), b) group 2 (female at 24 weeks), c) group 4 (female at 4 weeks) showed fatty change (small arrows) and mild necroinflammation (block arrow), d) group 4 (female at 8 weeks) showed only fatty change, e) group 5 (female at 4 weeks) and f) group 5 (female at 8 weeks)

APPENDIX B

Custom-made Diet

Procedure

1. Ingredient of diet (100 calories):

    60 g of pumpkin

    5 egg white only

    12.5 g of sugar

    21 ml of corn oil

    31.8 g of wheat flour

2. All ingredients of diet were mixed in a pot and baked for 20 minutes.

3. After cooling at room temperature, diet was cut into small pieces.

This diet contains 35% of energy from fat, 18% from protein and 47% from carbohydrate.

The Solutions for Western Blotting

1. Lysis buffer (Fresh preparation)

    0.01 M Tris pH 7.4

    0.15 M NaCl

    0.001 M EDTA

    1% Triton-X100

    Protease inhibotor cocktail (Sigma, USA)

    Phosphatase inhibitor cocktail 2 (Sigma, USA)

2. 30% Acrylamide/0.8% bisacrylamide (Dark bottle)

3. 1.5 M Tris pH 8.8

4. 0.5 M Tris pH6.8

5. 10% SDS

6. 10% Ammonium persulfae (10% AP) (Fresh preparation on ice)

7. TEMED

8. Sample buffer (2X) (Storage at -20^{0}C)

125 mM Tris pH 6.8

20% Glycerol

0.01% Bromophenol blue

200 mM DTT

9. Running buffer pH 8.3 (5X) 1 liter

Tris	15.1 g
Glycine	72.0 g
SDS	5.0 g

All reagents were dissolved in 900 ml dH_2O and adjusted the pH to 8.3 with conc. HCl. Then, the volume was adjusted to 1 liter.

10. Transfer buffer (1X) 1 liter

Tris	2.42 g
Glycine	11.24 g

All reagents were dissolved in 700 ml dH_2O and the volume was adjusted to 800 ml. Then, 200 ml 100% Methanol was added.

11. TBS pH 7.6 1 liter

1 M Tris pH 7.6	20 ml
NaCl	8 g

All reagents were dissolved in 900 ml dH_2O and the volume was adjusted to 1 liter.

12. Wash buffer pH 7.6 1 liter

TBS pH 7.6	999 ml
Tween 20	1 ml

13. Stripping buffer

0.2 M NaOH

14. SDS- polyacrylamide gel electrophoresis:

Reagents	10% Separating gel (ml)	5% Stacking gel (ml)
dH_2O	4.0	2.7
30% Acrylamide	3.3	0.67
1.5 M Tris pH 8.8	2.5	-
0.5 M Tris pH 6.8	-	0.5
10% SDS	0.1	0.04
10% AP*	0.1	0.04
TEMED*	0.004	0.004

* Quickly add solution and fill solution into glass plate assembly

APPENDIX C

Descriptives

		N	Mean	Std. Deviation	Std. Error	95% Confidence Interval for Mean		Minimum	Maximum
						Lower Bound	Upper Bound		
Starting BW	1	8	216.6250	6.73875	2.38251	210.9913	222.2587	202.00	225.00
	2	8	220.5000	11.61280	4.10575	210.7915	230.2085	202.00	240.00
	3	6	220.0000	1.67332	.68313	218.2440	221.7560	217.00	222.00
	4	7	214.4286	6.13344	2.31822	208.7561	220.1011	205.00	223.00
	Total	29	217.8621	7.74469	1.43815	214.9161	220.8080	202.00	240.00
Final BW	1	8	246.6250	7.90908	2.79628	240.0128	253.2372	232.00	259.00
	2	8	212.0000	33.37236	11.79891	184.1000	239.9000	166.00	262.00
	3	6	248.6667	14.43145	5.89161	233.5218	263.8115	236.00	275.00
	4	7	254.4286	13.56290	5.12630	241.8850	266.9722	237.00	277.00
	Total	29	239.3793	25.97996	4.82436	229.4971	249.2616	166.00	277.00

1=Control, 2=Alcohol, 3=Alcohol+curl, 4=Alcohol+curlI

ANOVA

		Sum of Squares	df	Mean Square	F	Sig.
Starting BW	Between Groups	177.859	3	59.286	.987	.415
	Within Groups	1501.589	25	60.064		
	Total	1679.448	28			
Final BW	Between Groups	8519.905	3	2839.968	6.841	.002
	Within Groups	10378.923	25	415.157		
	Total	18898.828	28			

Multiple Comparisons Tukey HSD

Starting BW	(I) GROUP	(J) GROUP	Mean Difference (I-J)	Std. Error	Sig.	95% Confidence Interval	
						Lower Bound	Upper Bound
	1	2	-3.8750	3.87503	.751	-14.5338	6.7838
		3	-3.3750	4.18552	.851	-14.8879	8.1379
		4	2.1964	4.01104	.946	-8.8365	13.2294
	2	1	3.8750	3.87503	.751	-6.7838	14.5338
		3	.5000	4.18552	.999	-11.0129	12.0129
		4	6.0714	4.01104	.445	-4.9615	17.1044
	3	1	3.3750	4.18552	.851	-8.1379	14.8879
		2	-.5000	4.18552	.999	-12.0129	11.0129
		4	5.5714	4.31174	.576	-6.2886	17.4315
	4	1	-2.1964	4.01104	.946	-13.2294	8.8365
		2	-6.0714	4.01104	.445	-17.1044	4.9615
		3	-5.5714	4.31174	.576	-17.4315	6.2886

* The mean difference is significant at the .05 level, 1=Control, 2=Alcohol, 3=Alcohol+curl, 4=Alcohol+curlI

Multiple Comparisons Tukey HSD

Final BW	(I) GROUP	(J) GROUP	Mean Difference (I-J)	Std. Error	Sig.	95% Confidence Interval	
						Lower Bound	Upper Bound
	1	2	34.6250(*)	10.18770	.011	6.6023	62.6477
		3	-2.0417	11.00397	.998	-32.3097	28.2263
		4	-7.8036	10.54527	.880	-36.8099	21.2027
	2	1	-34.6250(*)	10.18770	.011	-62.6477	-6.6023
		3	-36.6667(*)	11.00397	.013	-66.9347	-6.3987
		4	-42.4286(*)	10.54527	.002	-71.4349	-13.4223
	3	1	2.0417	11.00397	.998	-28.2263	32.3097
		2	36.6667(*)	11.00397	.013	6.3987	66.9347
		4	-5.7619	11.33583	.956	-36.9427	25.4189
	4	1	7.8036	10.54527	.880	-21.2027	36.8099
		2	42.4286(*)	10.54527	.002	13.4223	71.4349
		3	5.7619	11.33583	.956	-25.4189	36.9427

* The mean difference is significant at the .05 level, 1=Control, 2=Alcohol, 3=Alcohol+curl, 4=Alcohol+curlI

Descriptives

MDA	N	Mean	Std. Deviation	Std. Error	95% Confidence Interval for Mean		Minimum	Maximum
					Lower Bound	Upper Bound		
1	8	1.4425	.23505	.08310	1.2460	1.6390	1.18	1.81
2	8	3.4162	1.36041	.48098	2.2789	4.5536	1.86	5.20
3	6	1.4283	.14162	.05782	1.2797	1.5770	1.19	1.60
4	7	1.4271	.28611	.10814	1.1625	1.6917	1.05	1.78
Total	29	1.9803	1.14506	.21263	1.5448	2.4159	1.05	5.20

1=Control, 2=Alcohol, 3=Alcohol+curl, 4=Alcohol+curlI

ANOVA

MDA	Sum of Squares	df	Mean Square	F	Sig.
Between Groups	22.779	3	7.593	13.624	.000
Within Groups	13.933	25	.557		
Total	36.712	28			

Multiple ComparisonsTukey HSD

MDA		Mean Difference (I-J)	Std. Error	Sig.	95% Confidence Interval	
(I) group	(J) group				Lower Bound	Upper Bound
1	2	-1.97375*	.37327	.000	-3.0005	-.9470
	3	.01417	.40318	1.000	-1.0948	1.1232
	4	.01536	.38637	1.000	-1.0474	1.0781
2	1	1.97375*	.37327	.000	.9470	3.0005
	3	1.98792*	.40318	.000	.8789	3.0969
	4	1.98911*	.38637	.000	.9263	3.0519
3	1	-.01417	.40318	1.000	-1.1232	1.0948
	2	-1.98792*	.40318	.000	-3.0969	-.8789
	4	.00119	.41534	1.000	-1.1413	1.1436
4	1	-.01536	.38637	1.000	-1.0781	1.0474
	2	-1.98911*	.38637	.000	-3.0519	-.9263
	3	-.00119	.41534	1.000	-1.1436	1.1413

* The mean difference is significant at the .05 level, 1=Control, 2=Alcohol, 3=Alcohol+curl, 4=Alcohol+curlI

Descriptives

SOD	N	Mean	Std. Deviation	Std. Error	95% Confidence Interval for Mean		Minimum	Maximum
					Lower Bound	Upper Bound		
1	8	1.0814E3	145.00562	51.26723	960.1298	1202.5852	932.66	1359.37
2	8	1.1359E3	209.47760	74.06152	960.7298	1310.9852	893.03	1506.85
3	6	9.6628E2	139.44279	56.92728	819.9388	1112.6112	722.44	1113.89
4	7	9.6784E2	116.66166	44.09396	859.9460	1075.7340	827.44	1155.03
Total	29	1.0452E3	167.83385	31.16596	981.3405	1109.0216	722.44	1506.85

1=Control, 2=Alcohol, 3=Alcohol+curl, 4=Alcohol+curlI

ANOVA

SOD					
	Sum of Squares	df	Mean Square	F	Sig.
Between Groups	155476.087	3	51825.362	2.046	.133
Within Groups	633233.565	25	25329.343		
Total	788709.652	28			

Descriptives

Apoptosis		Mean	Std. Deviation	Std. Error	95% Confidence Interval for Mean		Minimum	Maximum
	N				Lower Bound	Upper Bound		
1	8	.3812	.28094	.09933	.1464	.6161	.00	.73
2	8	2.4325	2.67788	.94677	.1937	4.6713	.41	8.29
3	6	.9217	.73074	.29832	.1548	1.6885	.00	2.00
4	7	2.0843	2.35142	.88875	-.0904	4.2590	.39	7.31
Total	29	1.4700	1.96336	.36459	.7232	2.2168	.00	8.29

Mann-Whitney Test

Ranks

Apoptosis	group	N	Mean Rank	Sum of Ranks
	1	8	5.00	40.00
	2	8	12.00	96.00
	Total	16		

Test Statistics[b]

	Apoptosis
Mann-Whitney U	4.000
Wilcoxon W	40.000
Z	-2.943
Asymp. Sig. (2-tailed)	.003
Exact Sig. [2*(1-tailed Sig.)]	.002[a]
a. Not corrected for ties.	
b. Grouping Variable: group	

1=Control, 2=Alcohol, 3=Alcohol+curl, 4=Alcohol+curlI

Mann-Whitney Test

Ranks				
Apoptosis	group	N	Mean Rank	Sum of Ranks
	1	8	6.00	48.00
	3	6	9.50	57.00
	Total	14		

Test Statistics[b]	
	Apoptosis
Mann-Whitney U	12.000
Wilcoxon W	48.000
Z	-1.556
Asymp. Sig. (2-tailed)	.120
Exact Sig. [2*(1-tailed Sig.)]	.142[a]
a. Not corrected for ties.	
b. Grouping Variable: group	

1=Control, 3=Alcohol+curl

Mann-Whitney Test

Ranks				
	group	N	Mean Rank	Sum of Ranks
Apoptosis	1	8	5.00	40.00
	4	7	11.43	80.00
	Total	15		

Test Statistics[b]	
	Apoptosis
Mann-Whitney U	4.000
Wilcoxon W	40.000
Z	-2.780
Asymp. Sig. (2-tailed)	.005
Exact Sig. [2*(1-tailed Sig.)]	.004[a]
a. Not corrected for ties.	
b. Grouping Variable: group	

1=Control, 4=Alcohol+curII

Mann-Whitney Test

Ranks				
	group	N	Mean Rank	Sum of Ranks
Apoptosis	2	8	8.75	70.00
	3	6	5.83	35.00
	Total	14		

Test Statistics[b]	
	Apoptosis
Mann-Whitney U	14.000
Wilcoxon W	35.000
Z	-1.291
Asymp. Sig. (2-tailed)	.197
Exact Sig. [2*(1-tailed Sig.)]	.228[a]
a. Not corrected for ties.	
b. Grouping Variable: group	

2=Alcohol, 3=Alcohol+curl

Mann-Whitney Test

Ranks				
	group	N	Mean Rank	Sum of Ranks
Apoptosis	2	8	8.00	64.00
	4	7	8.00	56.00
	Total	15		

Test Statistics[b]	
	Apoptosis
Mann-Whitney U	28.000
Wilcoxon W	56.000
Z	.000
Asymp. Sig. (2-tailed)	1.000
Exact Sig. [2*(1-tailed Sig.)]	1.000[a]
a. Not corrected for ties.	
b. Grouping Variable: group	

2=Alcohol, 4=Alcohol+curII

Descriptives

NF-kB	N	Mean	Std. Deviation	Std. Error	95% Confidence Interval for Mean		Minimum	Maximum
					Lower Bound	Upper Bound		
1	8	.03975	.041348	.014619	.00518	.07432	.000	.107
2	8	1.07738	.517586	.182994	.64466	1.51009	.456	1.982
3	6	.15017	.022104	.009024	.12697	.17336	.119	.177
4	7	.16614	.087783	.033179	.08496	.24733	.095	.358
Total	29	.37934	.513733	.095398	.18393	.57476	.000	1.982

1=Control, 2=Alcohol, 3=Alcohol+curl, 4=Alcohol+curlI

ANOVA

NF-kB	Sum of Squares	df	Mean Square	F	Sig.
Between Groups	5.454	3	1.818	23.477	.000
Within Groups	1.936	25	.077		
Total	7.390	28			

Multiple Comparisons Tukey HSD

NF-kB		Mean Difference (I-J)	Std. Error	Sig.	95% Confidence Interval	
(I) group	(J) group				Lower Bound	Upper Bound
1	2	-1.037625*	.139137	.000	-1.42034	-.65491
	3	-.110417	.150285	.882	-.52380	.30296
	4	-.126393	.144021	.816	-.52254	.26976
2	1	1.037625*	.139137	.000	.65491	1.42034
	3	.927208*	.150285	.000	.51383	1.34059
	4	.911232*	.144021	.000	.51508	1.30738
3	1	.110417	.150285	.882	-.30296	.52380
	2	-.927208*	.150285	.000	-1.34059	-.51383
	4	-.015976	.154817	1.000	-.44182	.40987
4	1	.126393	.144021	.816	-.26976	.52254
	2	-.911232*	.144021	.000	-1.30738	-.51508
	3	.015976	.154817	1.000	-.40987	.44182

* The mean difference is significant at the .05 level, 1=Control, 2=Alcohol, 3=Alcohol+curl, 4=Alcohol+curlI

Descriptives

PPARr		Mean	Std. Deviation	Std. Error	95% Confidence Interval for Mean		Minimum	Maximum
	N				Lower Bound	Upper Bound		
1	8	.5662	.18531	.06552	.4113	.7212	.35	.81
2	8	.6800	.16169	.05717	.5448	.8152	.37	.94
3	6	.4350	.03146	.01285	.4020	.4680	.40	.49
4	7	.5386	.23184	.08763	.3242	.7530	.28	.84
Total	29	.5638	.18544	.03444	.4933	.6343	.28	.94

1=Control, 2=Alcohol, 3=Alcohol+curI, 4=Alcohol+curII

ANOVA

PPARr	Sum of Squares	df	Mean Square	F	Sig.
Between Groups	.212	3	.071	2.354	.096
Within Groups	.751	25	.030		
Total	.963	28			

Descriptives

Alpha-SMA		Mean	Std. Deviation	Std. Error	95% Confidence Interval for Mean		Minimum	Maximum
	N				Lower Bound	Upper Bound		
1	8	.6100	.30388	.10744	.3560	.8640	.28	1.07
2	8	.6375	.15267	.05398	.5099	.7651	.32	.79
3	6	.7217	.26940	.10998	.4389	1.0044	.38	1.14
4	7	.6043	.24677	.09327	.3761	.8325	.40	1.02
Total	29	.6393	.23860	.04431	.5486	.7301	.28	1.14

1=Control, 2=Alcohol, 3=Alcohol+curl, 4=Alcohol+curlI

ANOVA

Alpha-SMA	Sum of Squares	df	Mean Square	F	Sig.
Between Groups	.056	3	.019	.304	.822
Within Groups	1.538	25	.062		
Total	1.594	28			

BIOGRAPHY

NAME	Miss Suchittra Samuhasaneeto
BIRTHDAY	July 11, 1980
PLACE OF BIRTH	Phatthalung, Thailand
EDUCATION	1999-2003 B.Sc. in Biology (First Class Honors), Faculty of Science, Prince of Songkla University 2003-2006 M.Sc. in Physiology, GPAX 3.81, Graduate School, Chulalongkorn University 2006-2009 Ph.D. candidate in Physiology, Graduate School, Chulalongkorn University
PUBLICATIONS	1.Thong-Ngam D, **Samuhasaneeto S**, Suyasunanon D, Wisedopas N. Development of a simple rat model of nonalcoholic steatohepatitis. Thai Journal of Gastroenterology 2005:6:3; 144-148. 2.Thong-Ngam D, **Samuhasaneeto S**, Kulaputana O, Patumraj S, Komolmitr P, Wisedopas N. Effects of n-acetylcysteine on change of oxidative stress and histopathology in rats with non-alcoholic steatohepatitis. Gastroenterology 2006:130:4; A594. 3.**Samuhasaneeto S**, Thong-Ngam D, Kulaputana O, Patumraj S, Klaikaew N. Effects of n-acetylcysteine on oxidative stress in rats with nonalcoholic steatohepatitis. Journal of the Medical Association of Thailand 2007:90:4; 788-797. 4.**Samuhasaneeto S**, Thong-Ngam D, Klaikaew N. Factors influencing a rat model of alcoholic liver disease for research. Thai Journal Physiological Sciences 2007:20:1; 13-18. 5.Thong-Ngam D, **Samuhasaneeto S**, Kulaputana O, Klaikaew N. N-acetylcysteine attenuates oxidative stress and liver pathology in rats with non-alcoholic steatohepatitis. World Journal of Gastroenterol 2007:13:38; 5127-5132. 6.**Samuhasaneeto S**, Thong-Ngam D, Kulaputana O, Klaikaew N. Effects of vitamin B6 supplement on serum transaminase and total glutathione in rats with nonalcoholic steatohepatitis (NASH). Thai Journal of Gastroenterology 2007:8:3; 119-122.